



# Polarimetric BSSRDF Acquisition of Dynamic Faces



Hyunho Ha    Inseung Hwang    Nestor Monzon    Jaemin Cho    Donggun Kim  
Seung-Hwan Baek    Adolfo Muñoz    Diego Gutierrez    Min H. Kim



Universidad  
Zaragoza

**POSTECH**

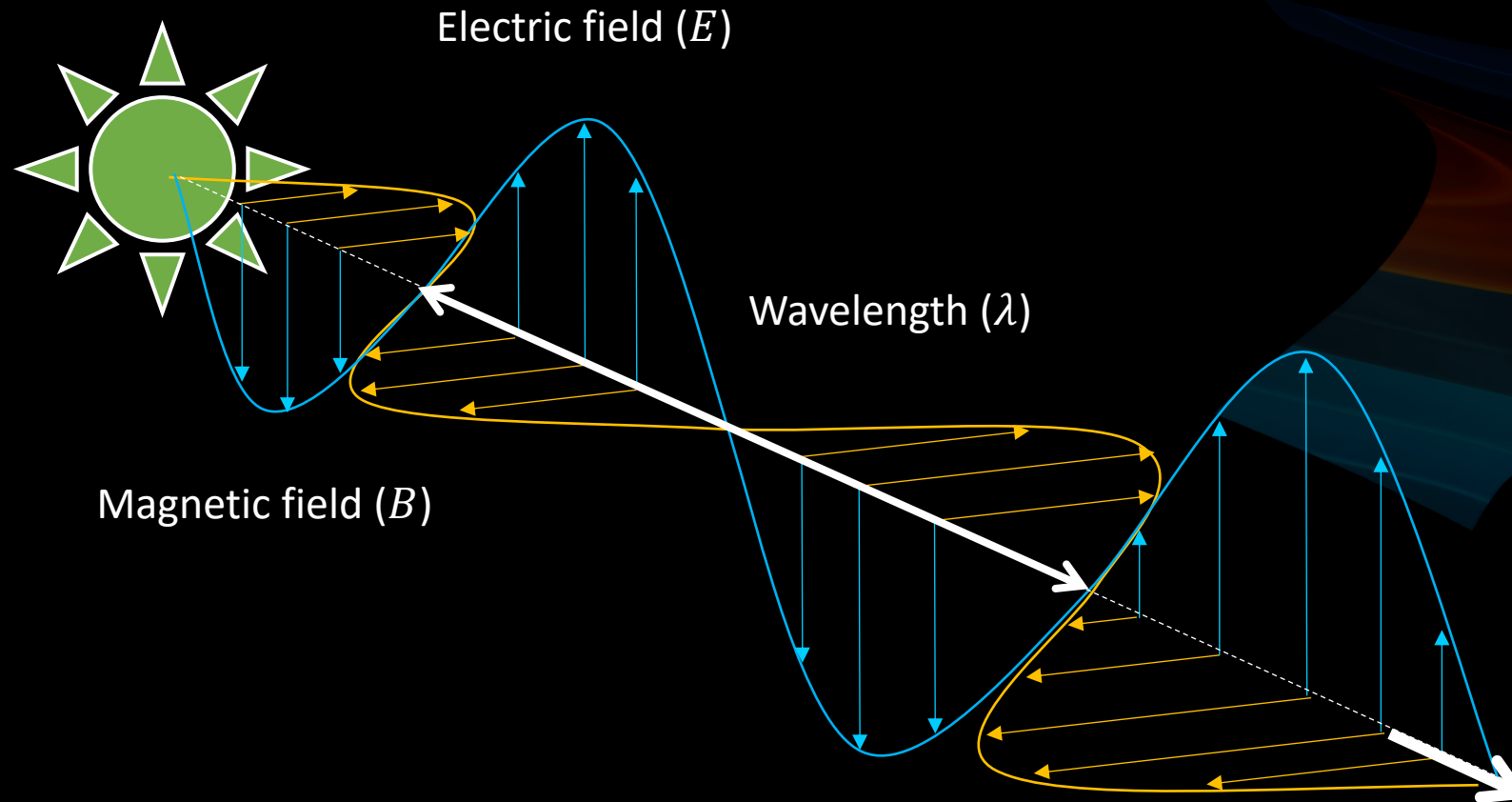
Sponsored by



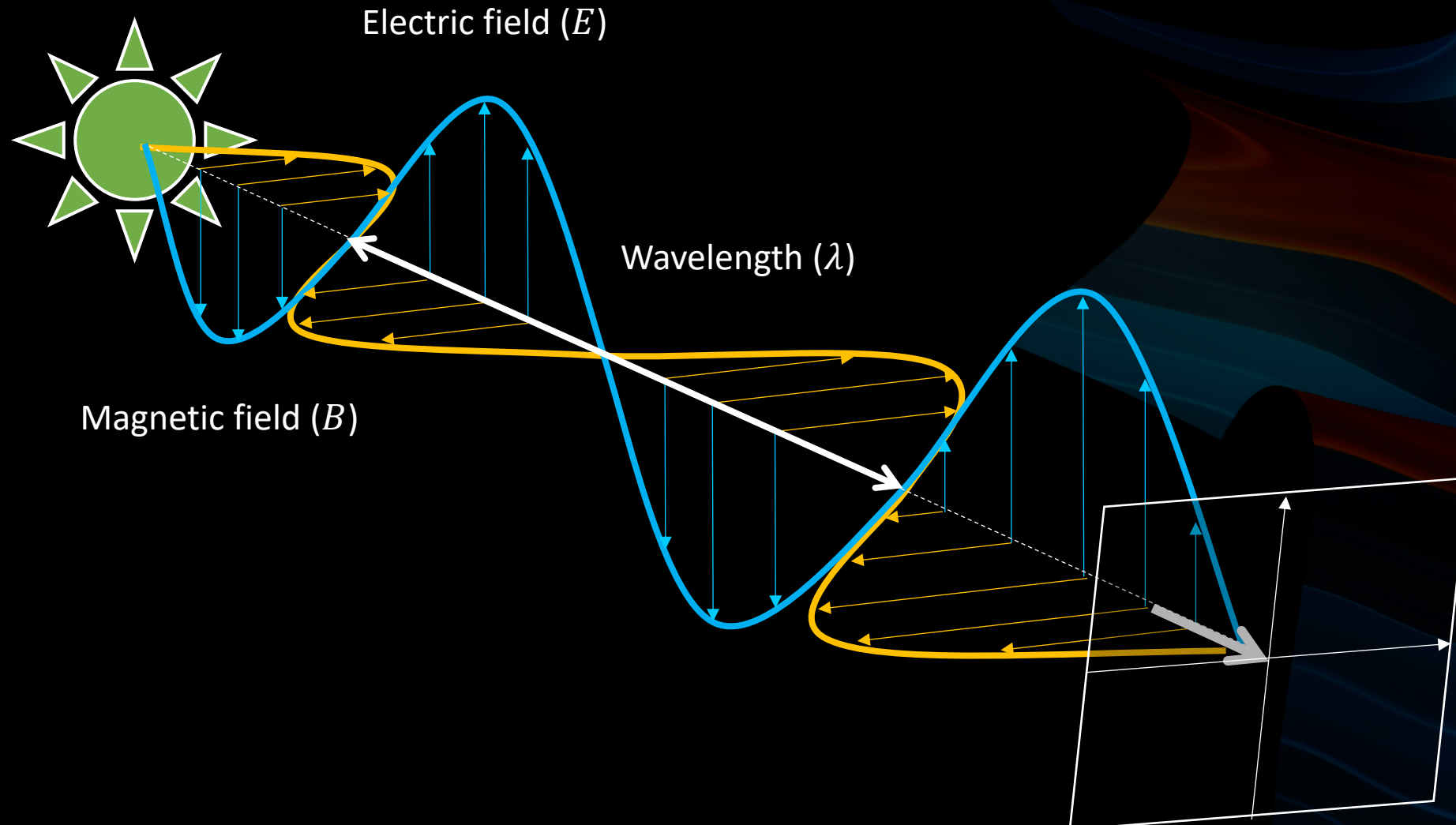
Organized by



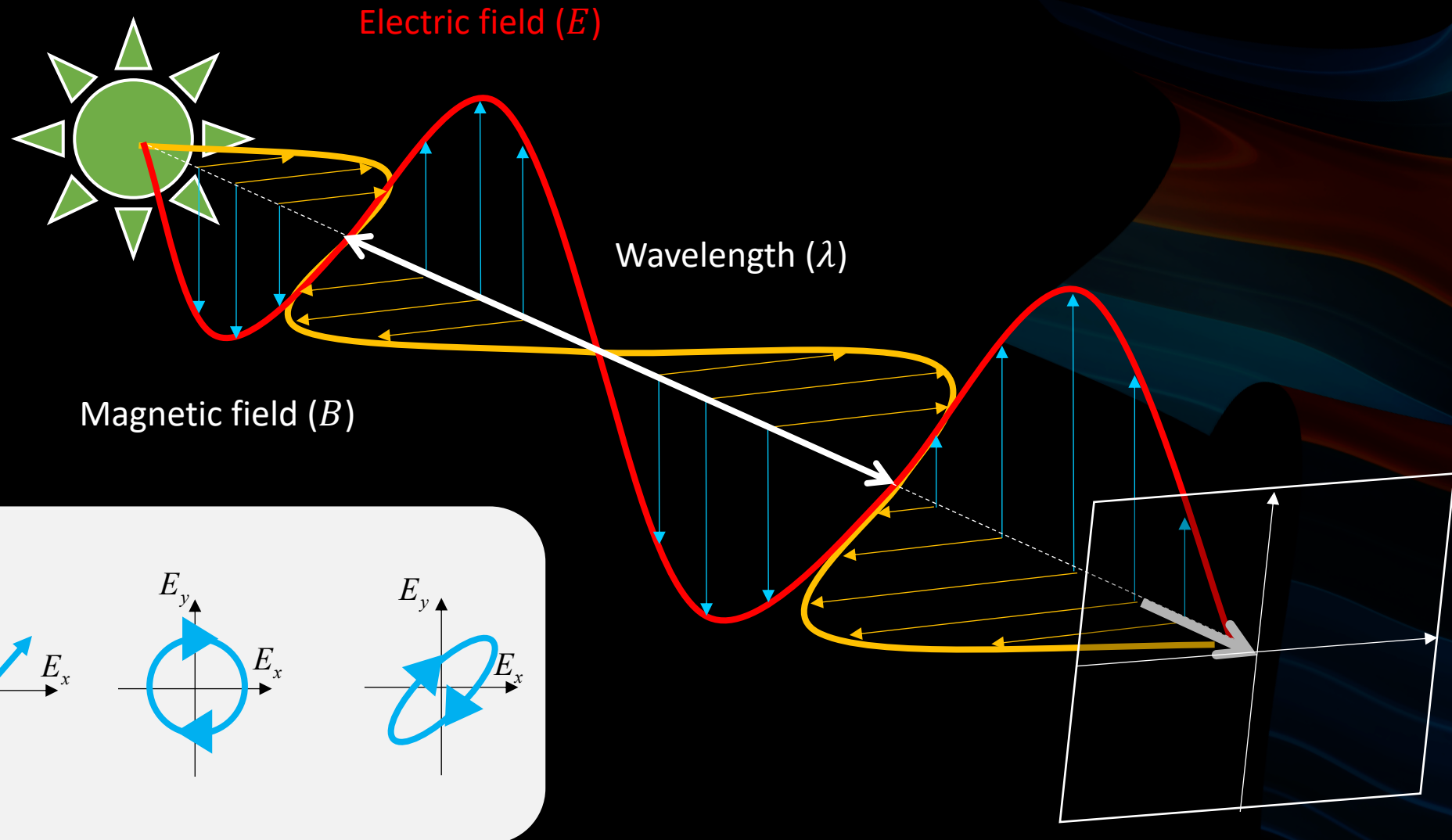
# Polarization



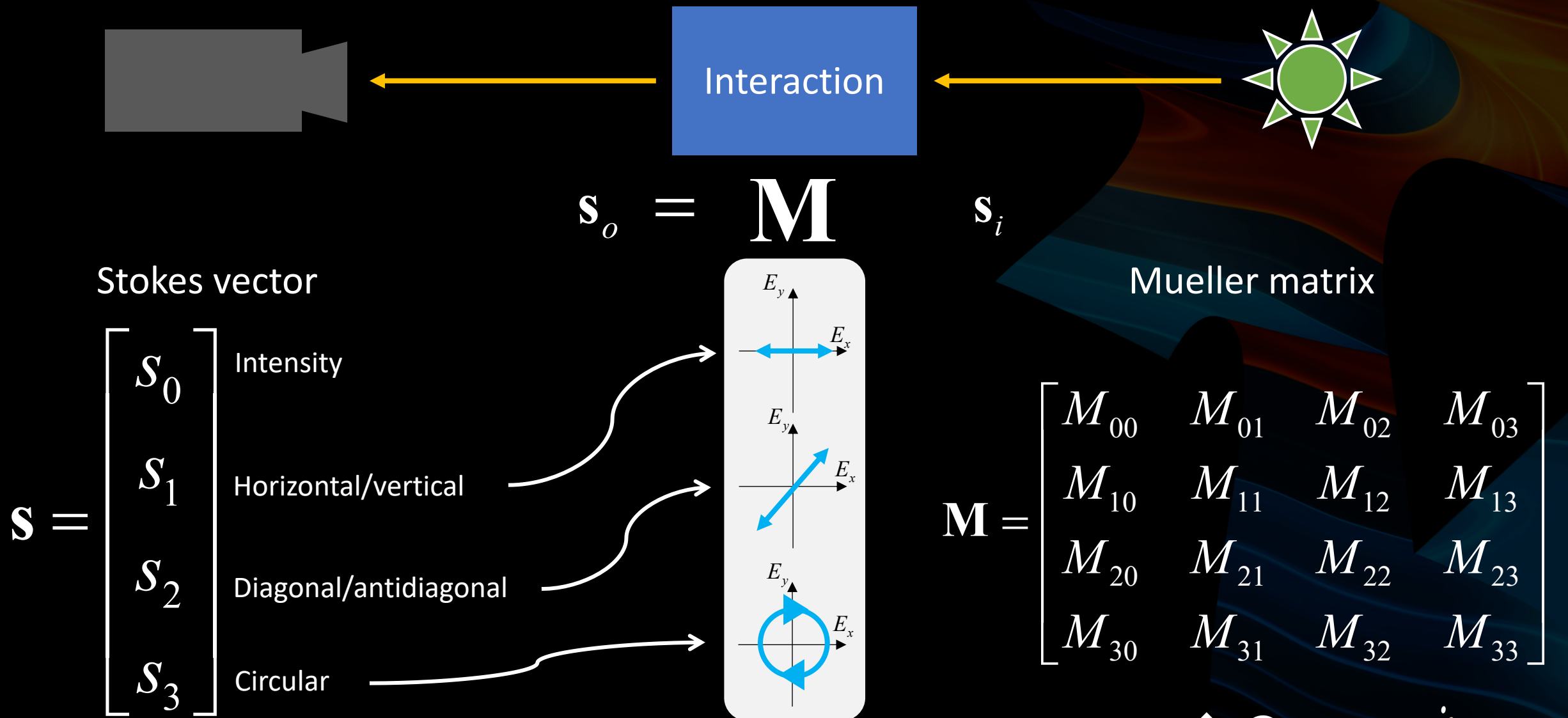
# Polarization



# Polarization



# Stokes Vector and Mueller Matrix



# Face Model



- Oiliness
  - Main specular reflection
- Outer layer
  - Epidermis + upper part of the dermis

$$\begin{array}{ccc} C_{h,out} & C_m & \beta_m \\ \text{Fraction of hemoglobin} & \text{Fraction of melanin} & \text{Fraction of eumelanin} \\ & & \text{in melanin} \\ \cdot \text{Inner layer} & \cdot \text{Lower part of the dermis} & \\ C_{h,in} & & \end{array}$$

Fraction of hemoglobin in inner layer

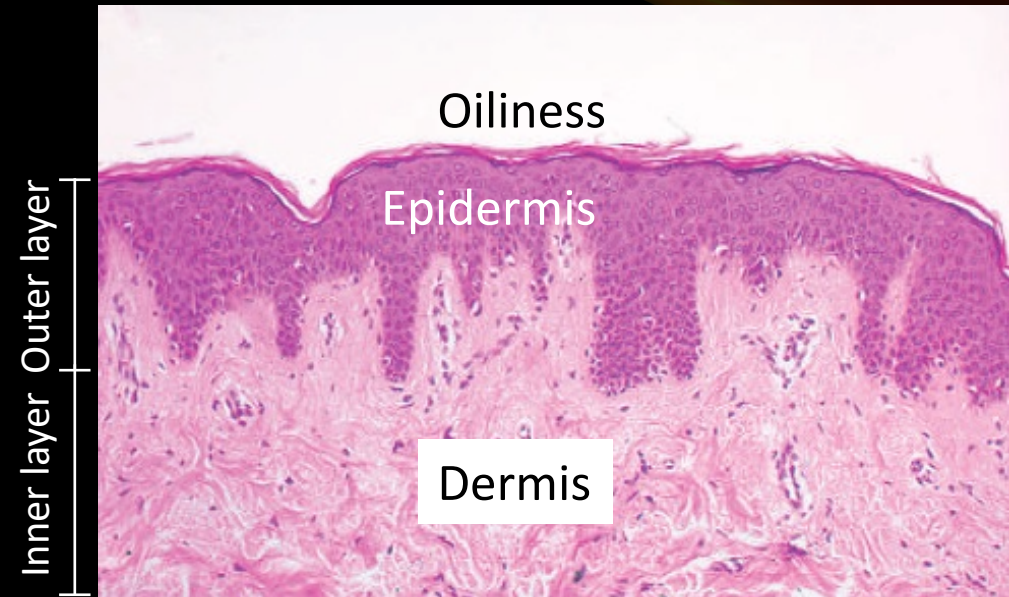
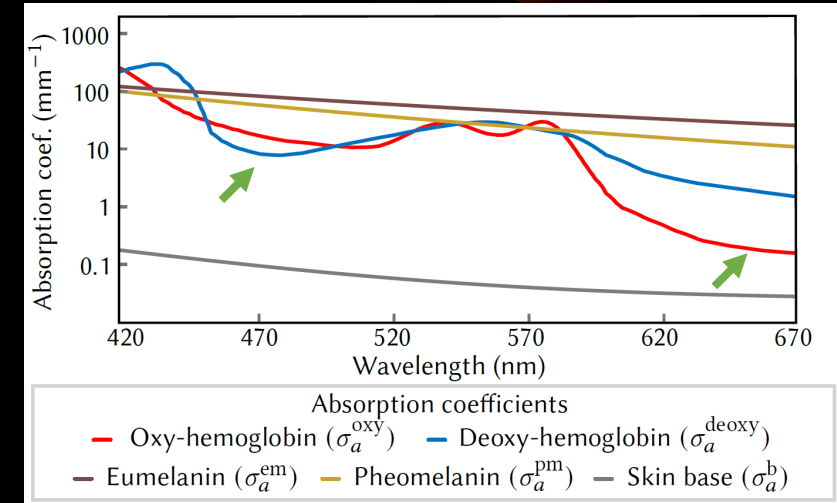


Figure from *Dermatology Lecture Notes*, Eleventh Edition.

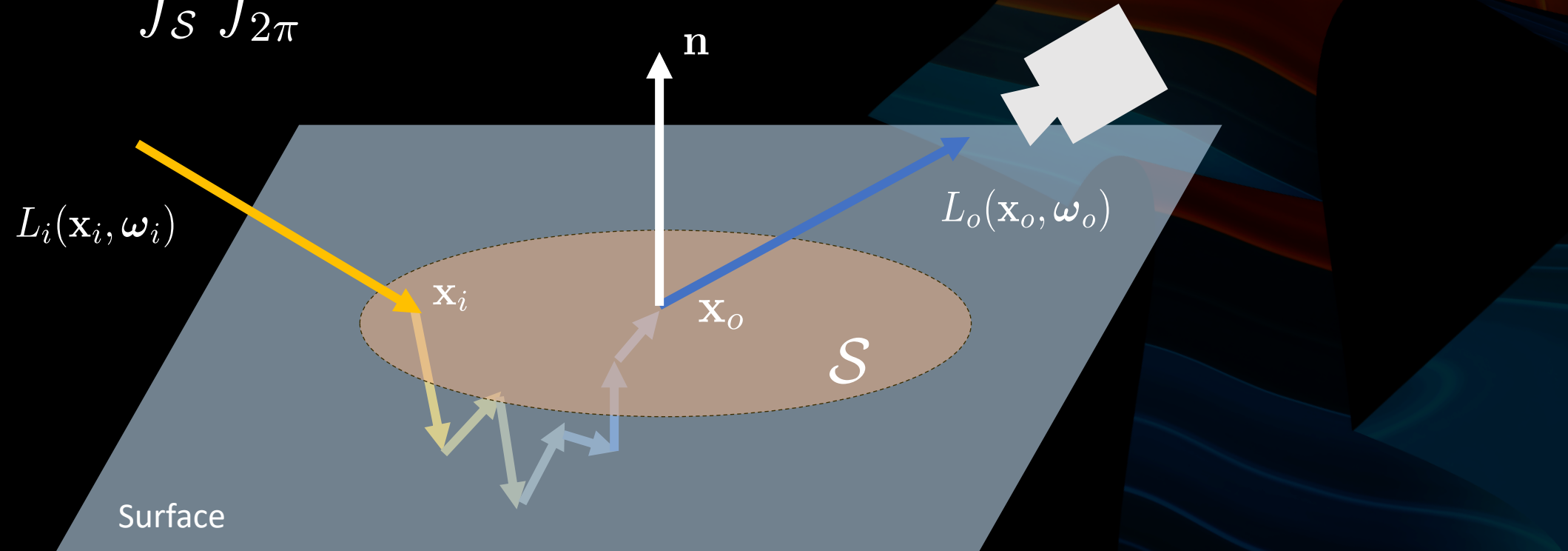


# Human Skin: Subsurface Scattering



- Bidirectional Subsurface Scattering Reflectance Distribution Function  $\Psi$

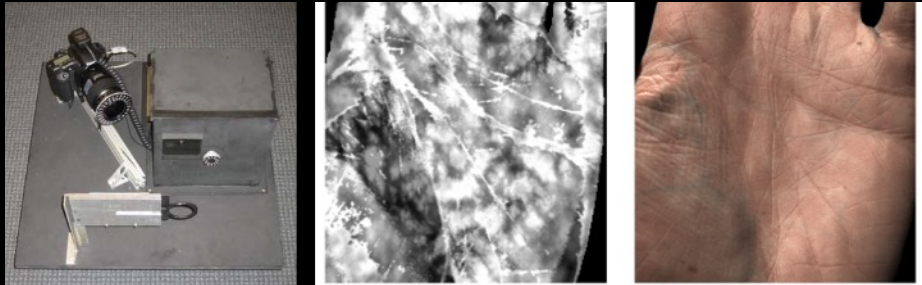
$$L_o(\mathbf{x}_o, \omega_o) = \int_{\mathcal{S}} \int_{2\pi} \Psi(\mathbf{x}_i, \omega_i; \mathbf{x}_o, \omega_o) L_i(\mathbf{x}_i, \omega_i) (\mathbf{n} \cdot \omega_i) d\omega_i d\mathcal{S}(\mathbf{x}_i)$$



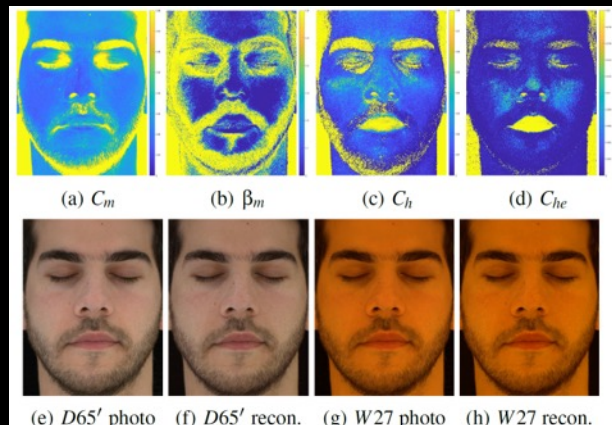
# Related Work



- Human face: beneath skin



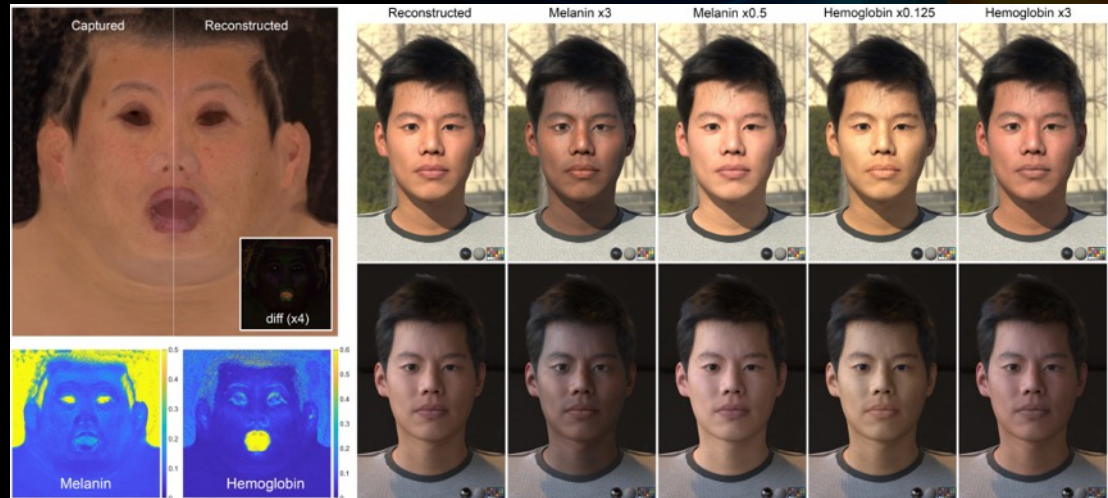
Donner et al. 2008



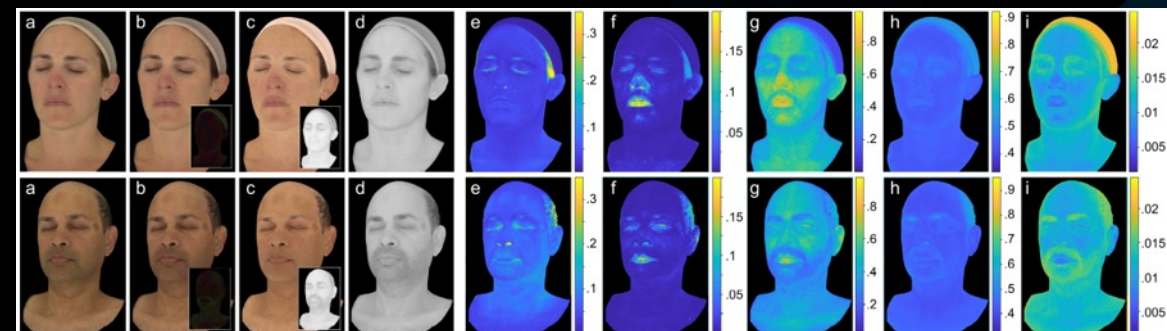
Gitlina et al. 2010



Jimenez et al. 2010

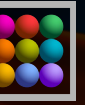


Aliaga et al. 2022



Aliaga et al. 2023

# Related Work



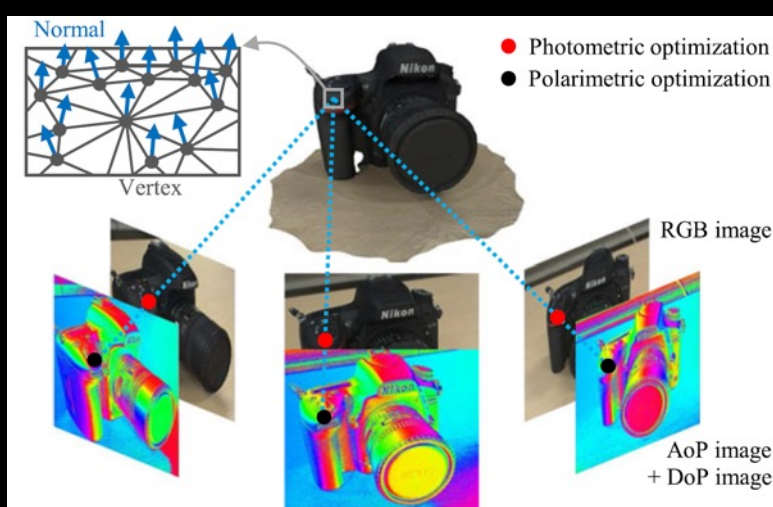
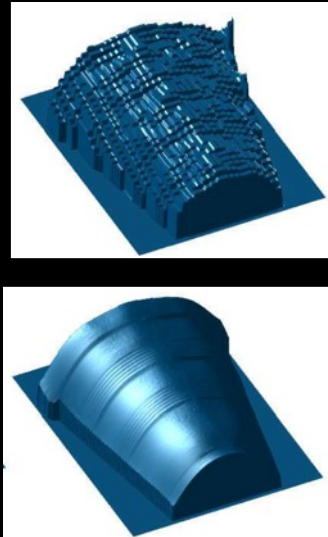
- Polarimetry



Ghosh et al. 2010

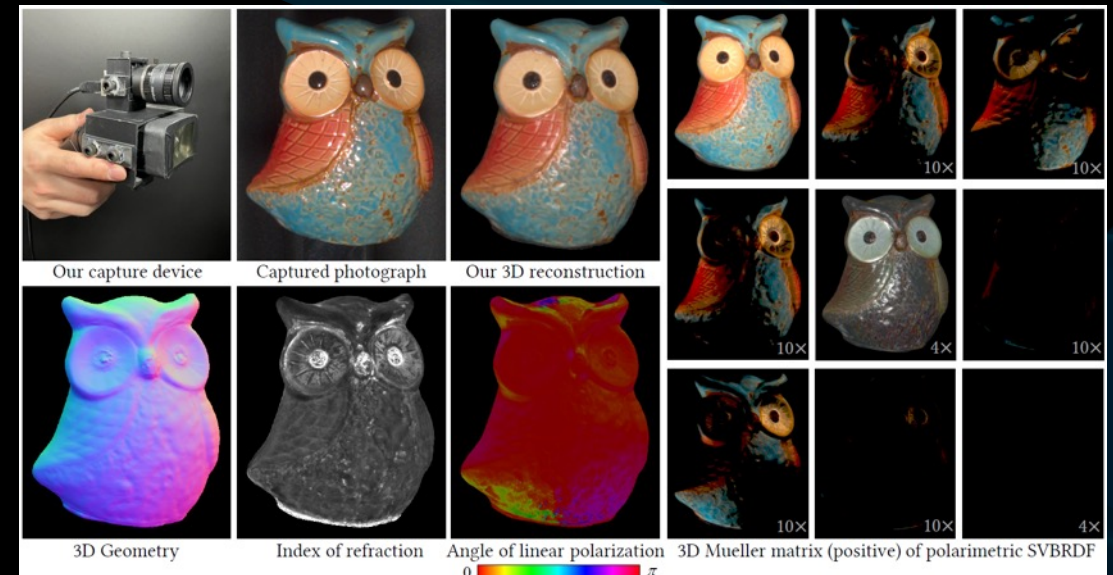


Baek et al. 2018



Kadambi et al. 2010

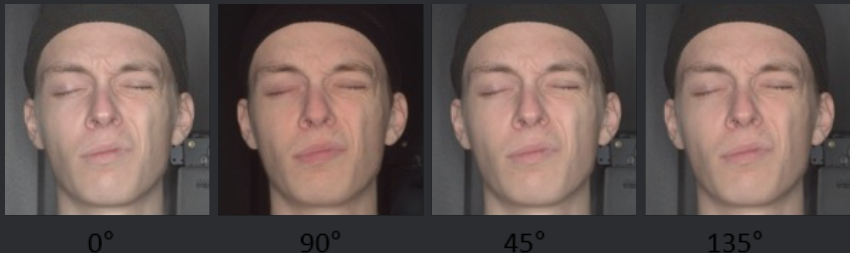
Zhao et al. 2020



Hwang et al. 2022



## Specular appearance



0°

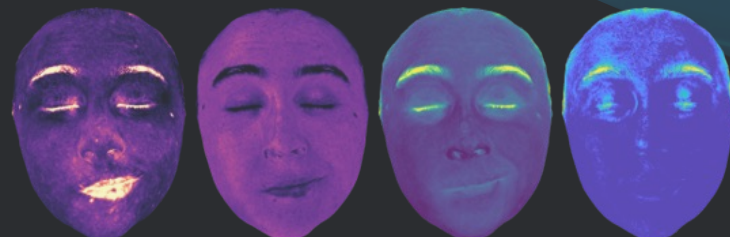
90°

45°

135°

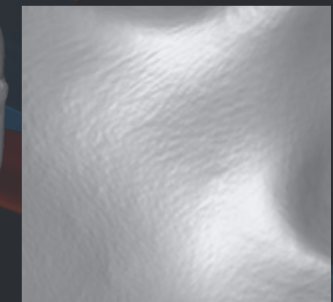
## Polarimetric reflectance

## Multispectral subsurface scattering



## Biophysical parameters

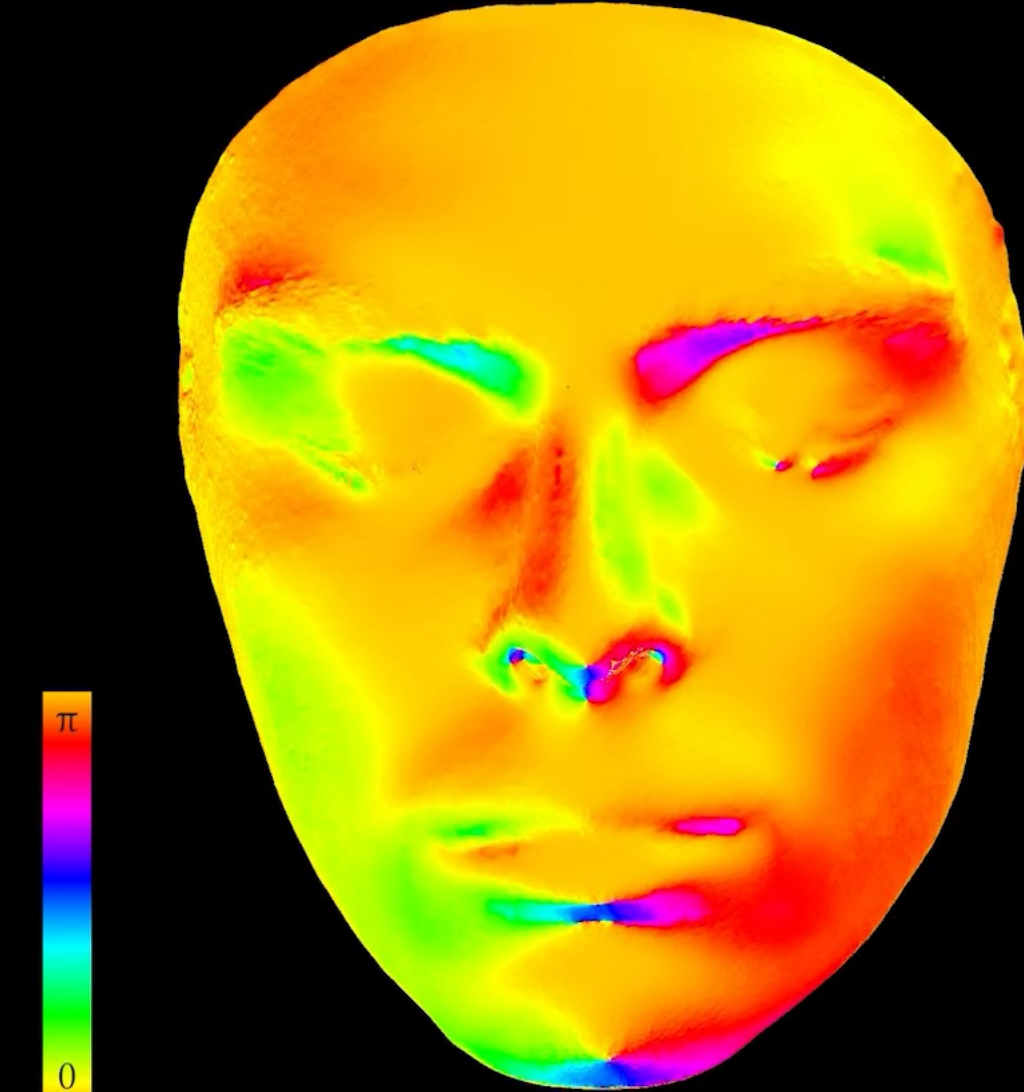
## Geometry



## Inverse rendering



Full rendering

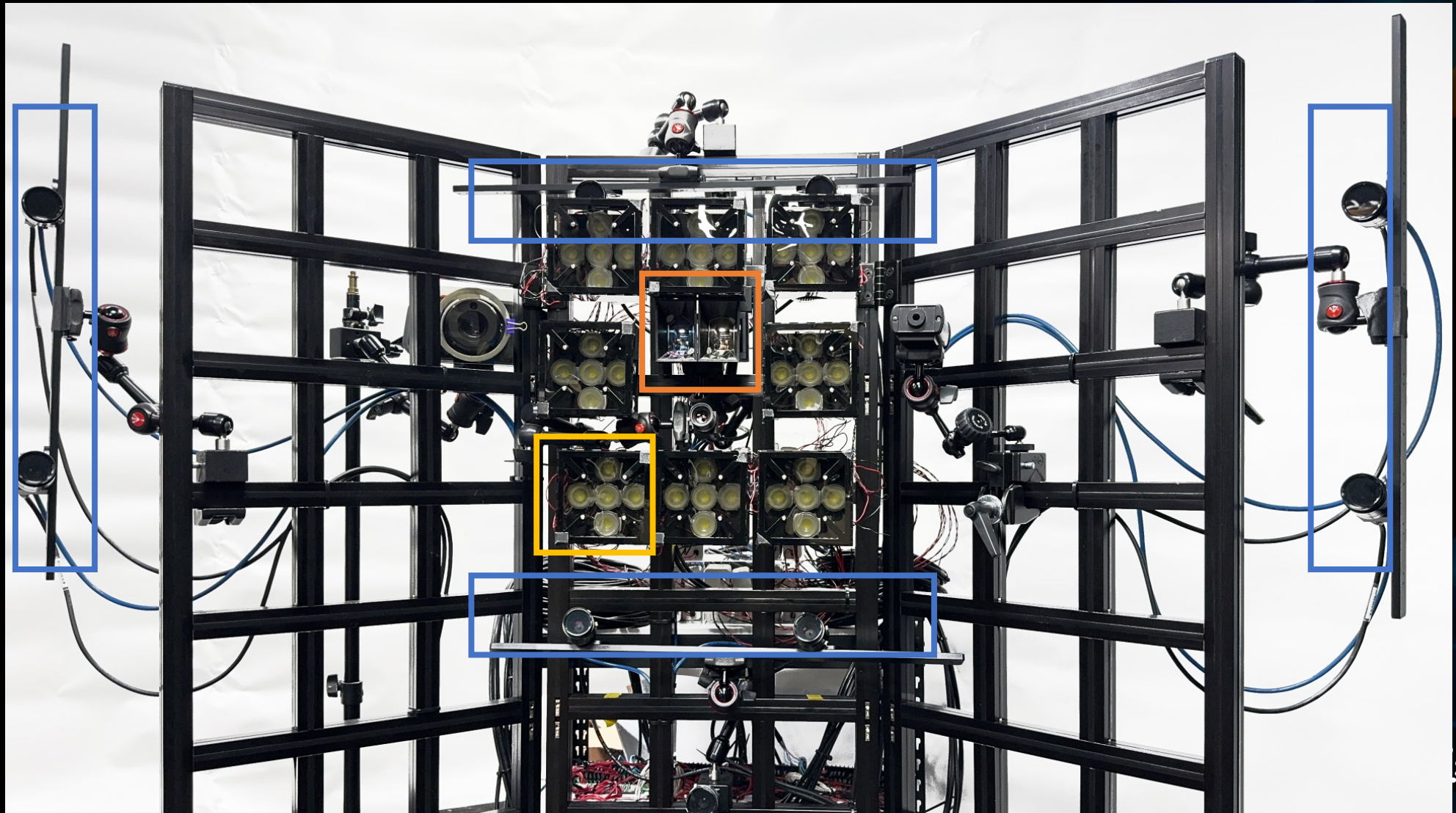


Angle of linear polarization

# Hardware



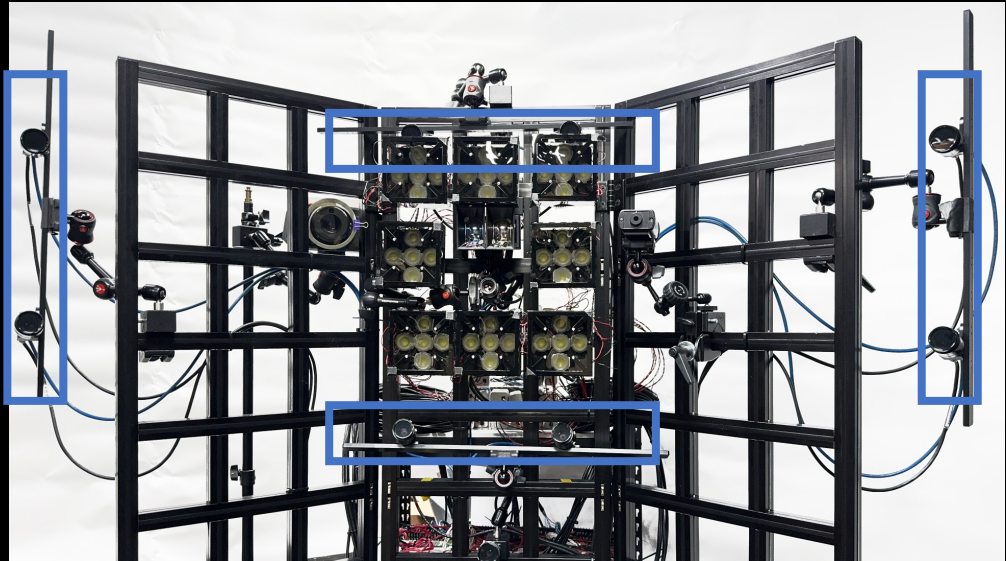
- Capture **multispectral polarimetric stereo images**



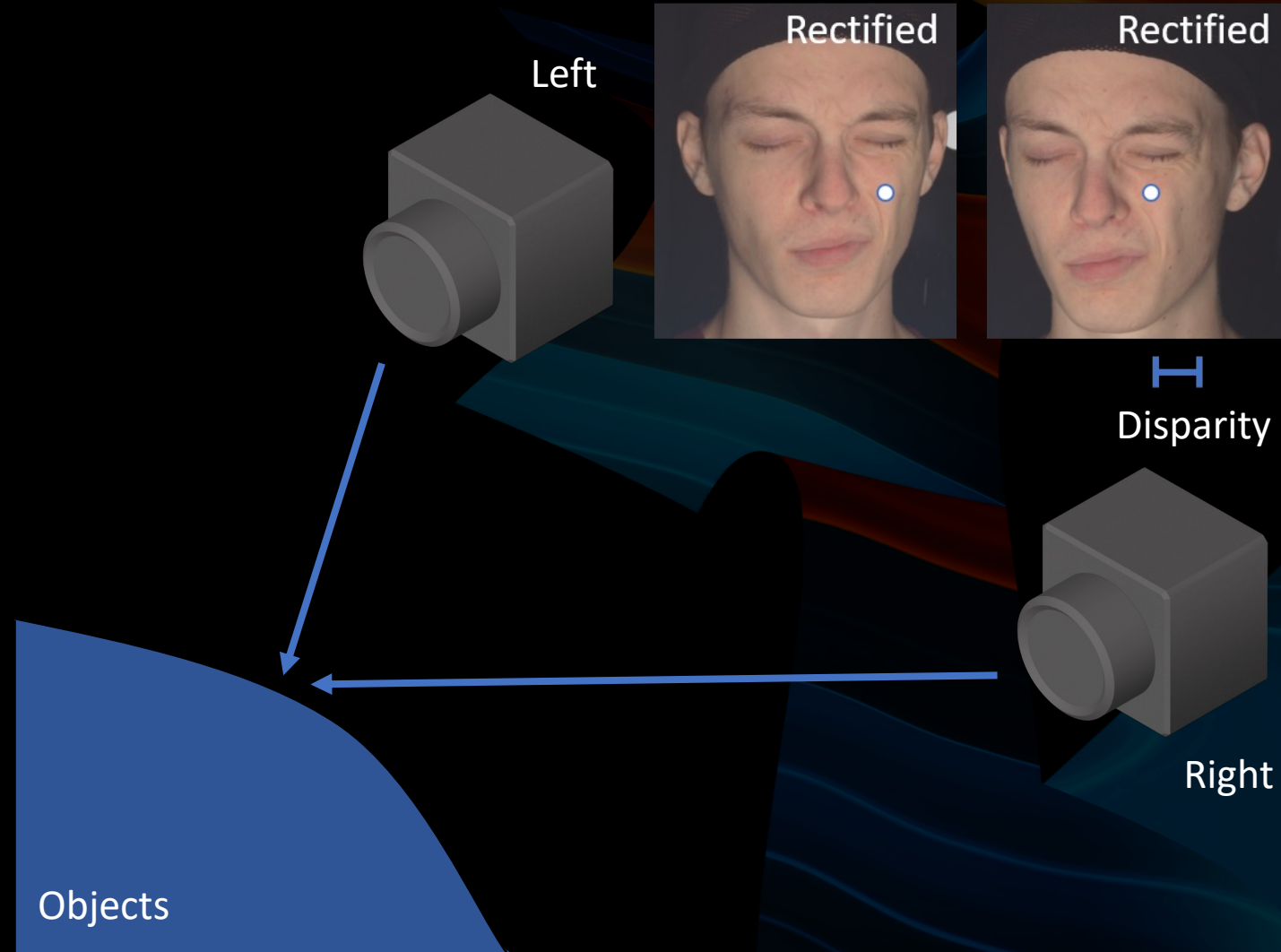
# Hardware: Stereo Imaging



## Geometric information



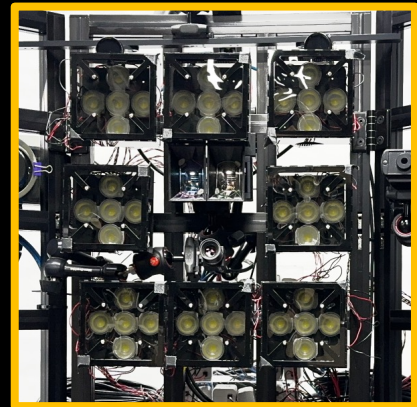
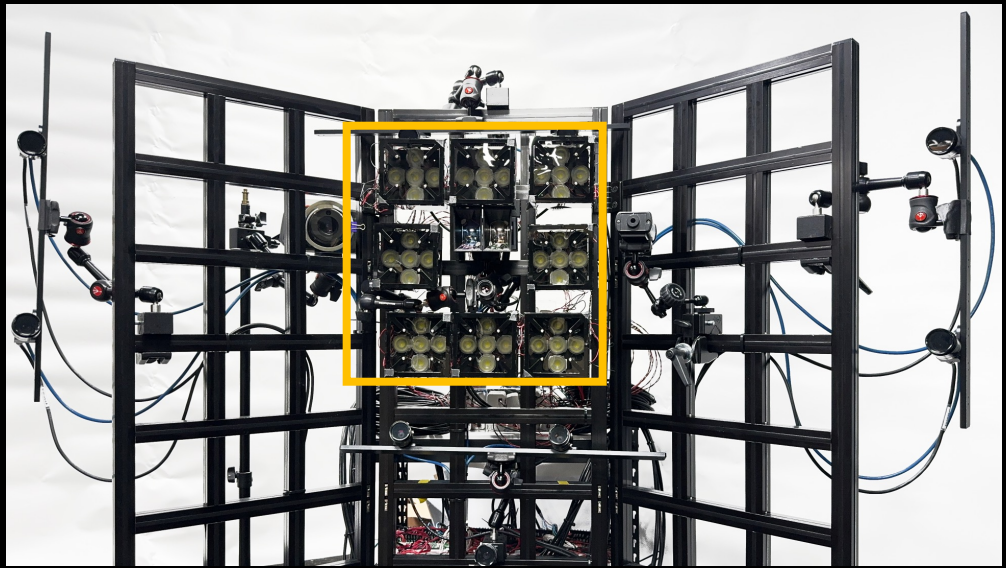
Two color machine vision cameras



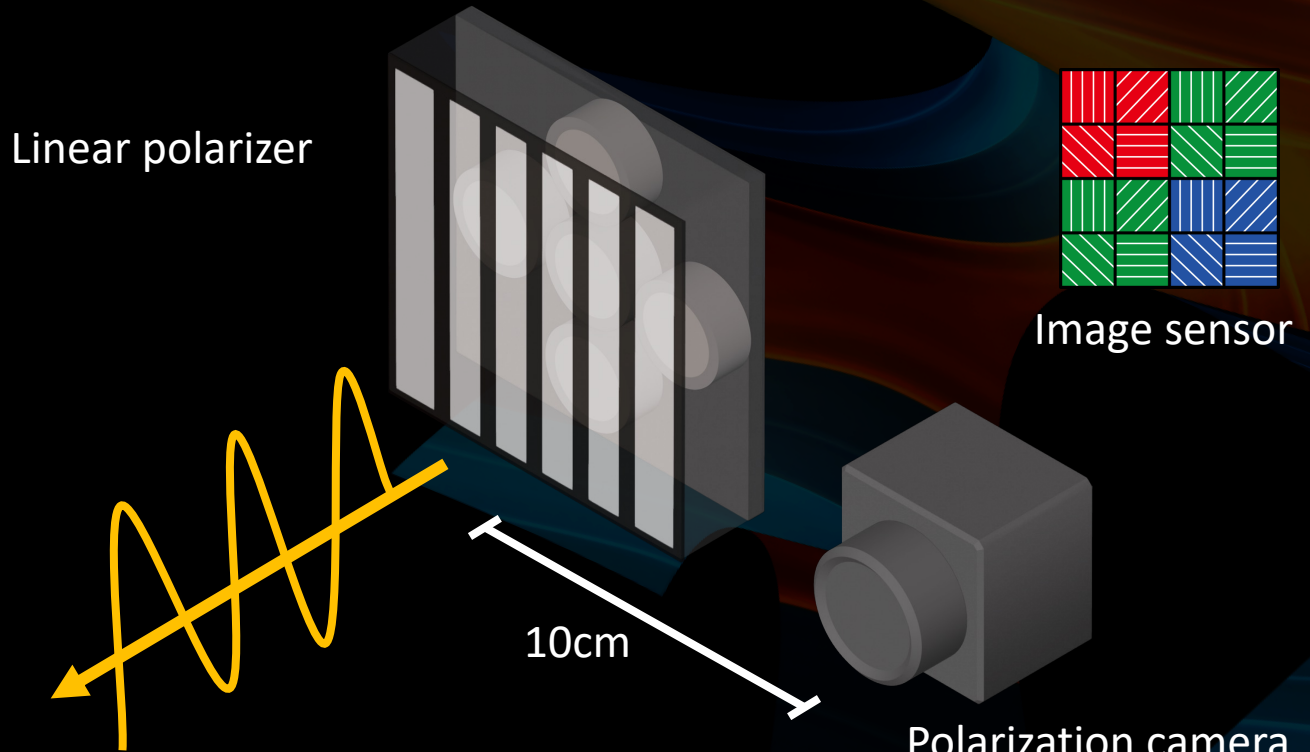
# Hardware: Polarimetric Imaging



## Polarimetric information



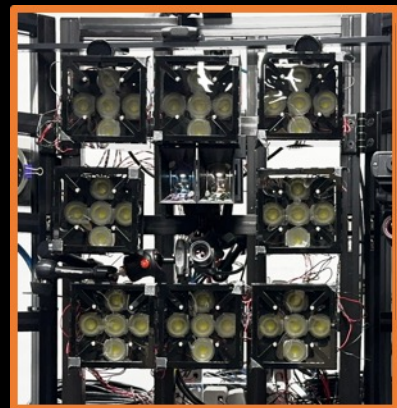
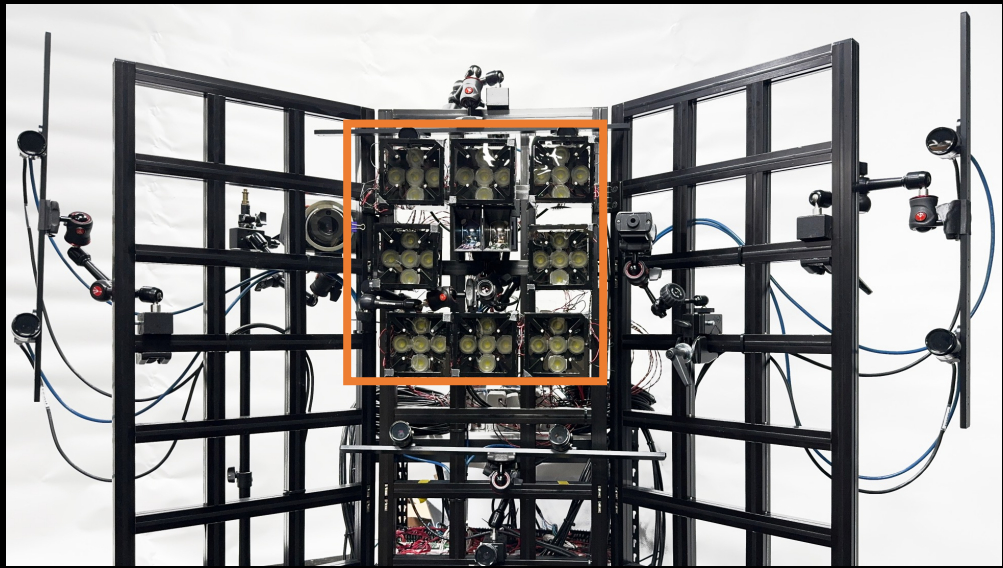
Polarization camera



# Hardware: Multispectral Imaging

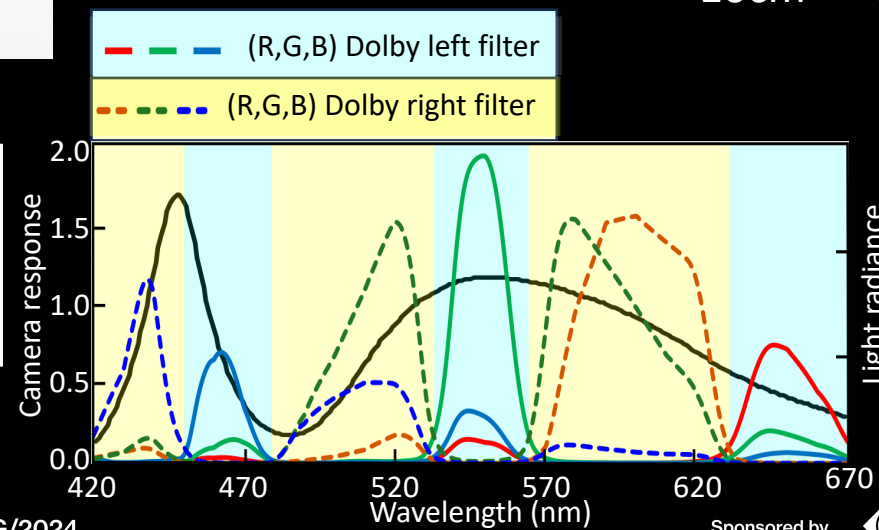
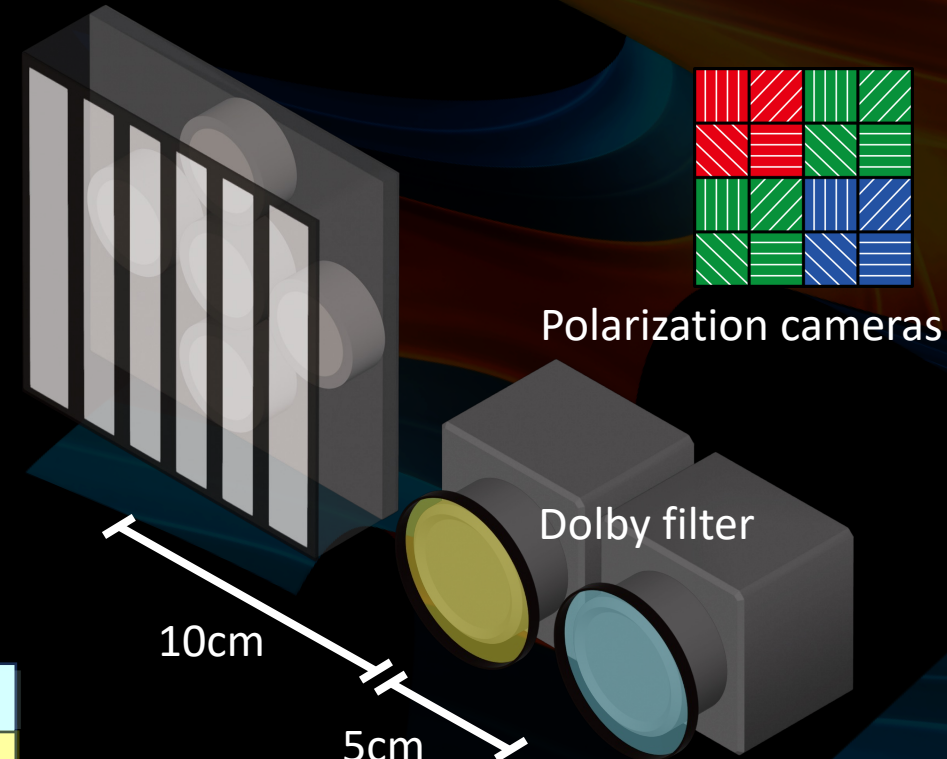


Spectral reflectance information



Dolby 3D glasses

Linear polarizer



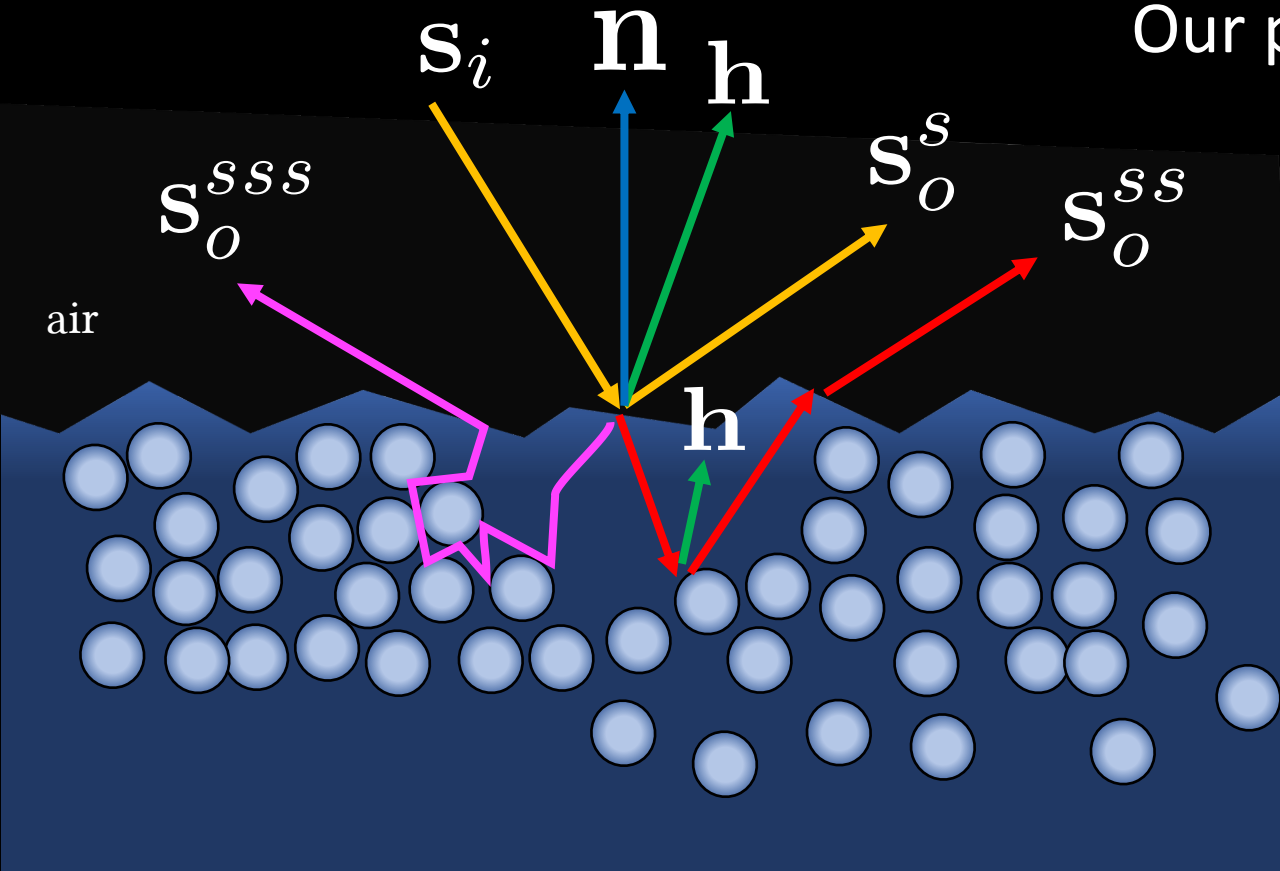
Dolby left

Dolby right

# Polarimetric Reflectance Model



$$\text{pBSSRDF: } \mathbf{S}_o = \mathbf{P}(\omega_i, \omega_o) \mathbf{S}_i$$

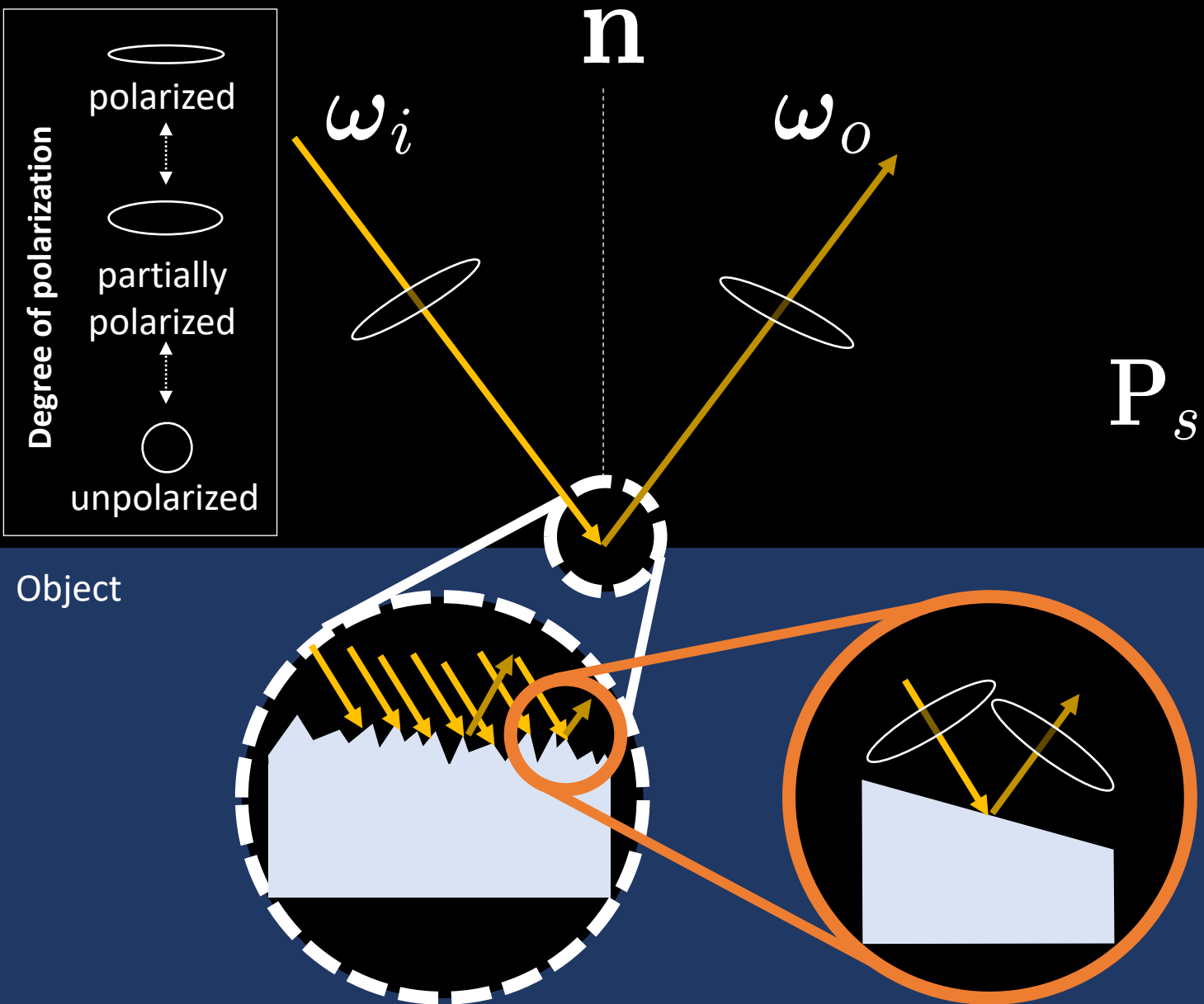


Our pBSSRDF includes 3 types of reflection

- Specular
- Single scattering
- Subsurface scattering

$$P = P_s + P_{ss} + P_{sss}$$

# Polarimetric BSSRDF: Specular



$$\mathbf{s}_o = \mathbf{P}(\omega_i, \omega_o) \mathbf{s}_i$$

Baek et al. 2018.

Coordinate conversion   Fresnel reflection   Coordinate conversion

$$P_s = \kappa_s C_{h \rightarrow o} F^R(\eta) C_{i \rightarrow h}$$

Refractive index

Specular roughness

Normal distribution function   Geometric shading

$$\kappa_s = \rho_s \frac{\mathcal{D}(\alpha_s) \mathcal{G}(\alpha_s)}{4(n \cdot \omega_i)(n \cdot \omega_o)}$$

Specular intensity

Normal

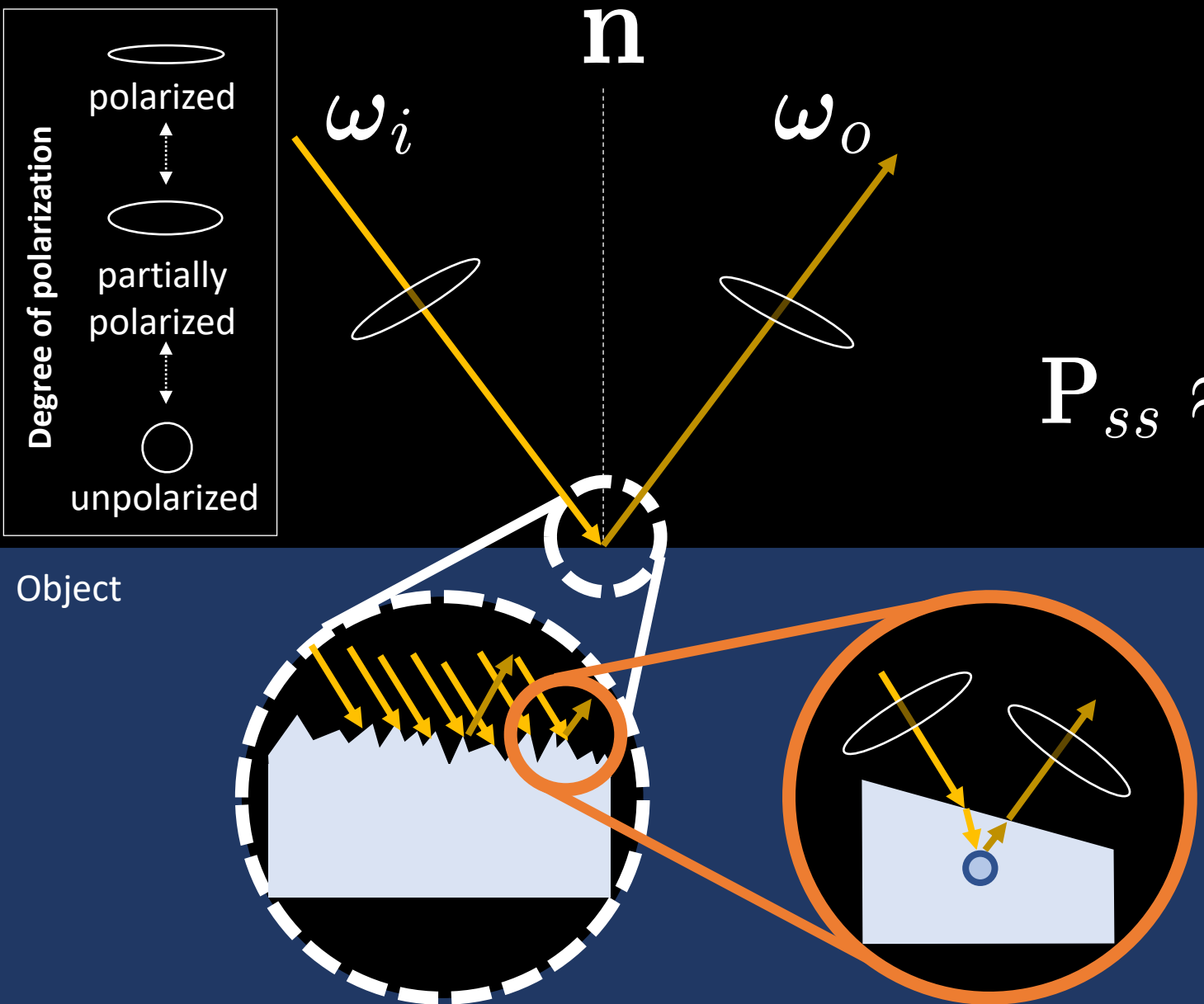
Sponsored by



Organized by



# Polarimetric BSSRDF: Single Scattering



**n**

$\omega_i$

$\omega_o$

$$P_{ss} \approx \kappa_{ss} C_{h \rightarrow o} F^R(\eta) C_{i \rightarrow h}$$

$$S_o = P(\omega_i, \omega_o) S_i$$

Hwang et al. 2022.

Coordinate conversion  
Fresnel reflection  
Coordinate conversion

$$C_{h \rightarrow o} F^R(\eta) C_{i \rightarrow h}$$

Refractive index

Single scat. roughness

Normal distribution function

$$\kappa_{ss} = \rho_{ss} \frac{D(\alpha_{ss}) G(\alpha_{ss})}{4(n \cdot \omega_i)(n \cdot \omega_o)}$$

Single Scat. intensity

Normal

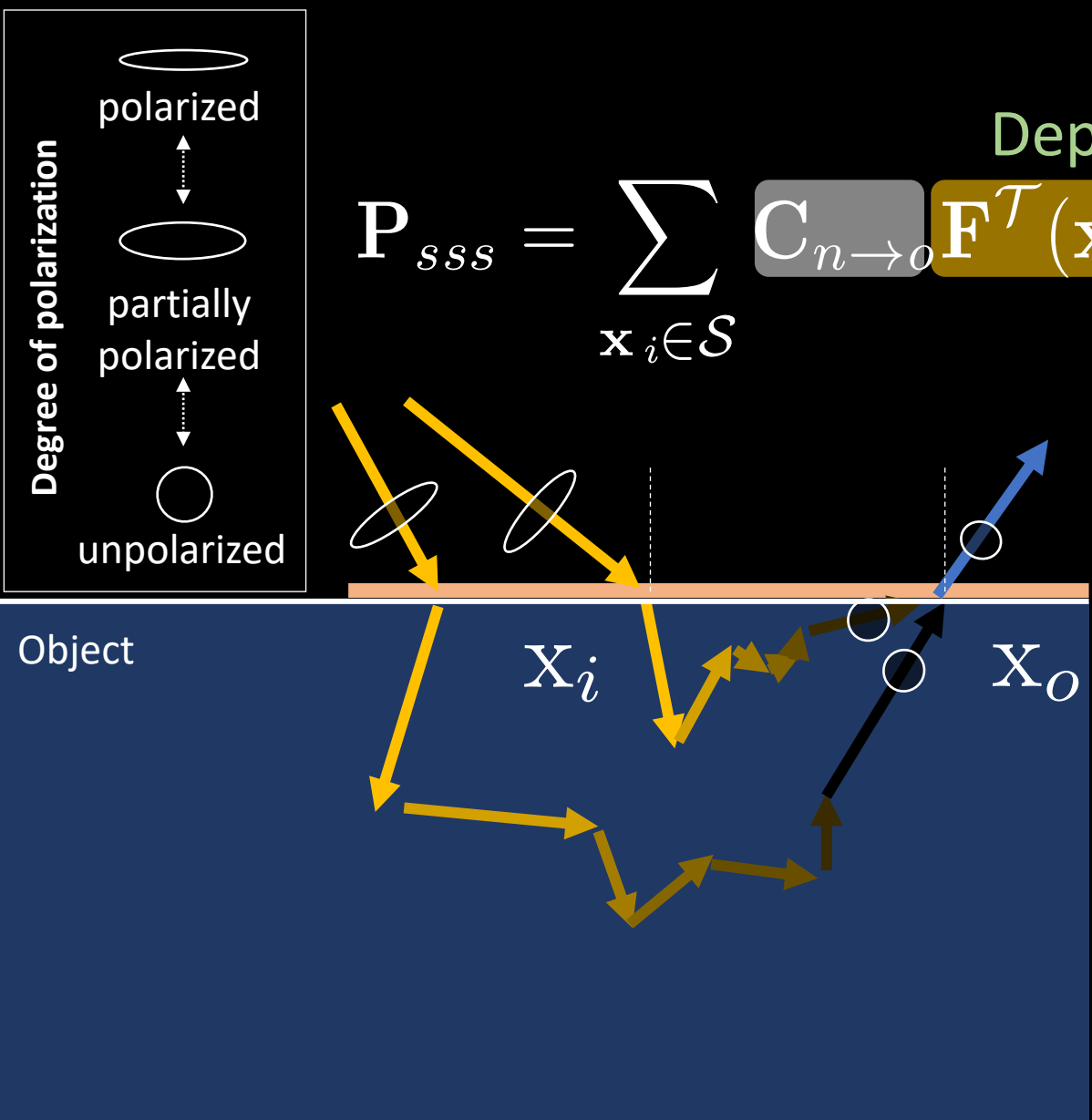
Sponsored by



Organized by



# Polarimetric BSSRDF: Subsurface Scattering



Depolarization

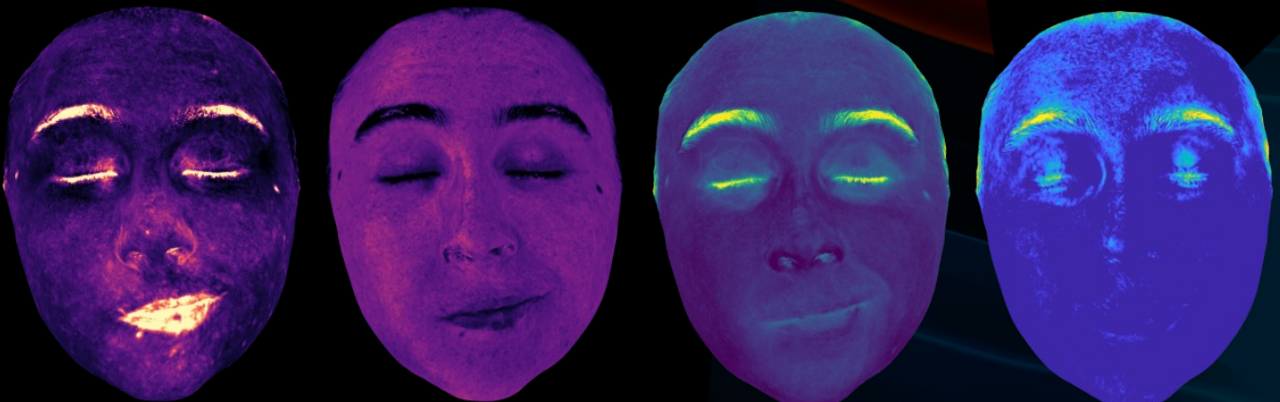
$$S_o = P(\omega_i, \omega_o) S_i$$

Fresnel transmittance

Subsurface scattering

Coordinate conversion

Biophysical Parameters



Sponsored by



Organized by

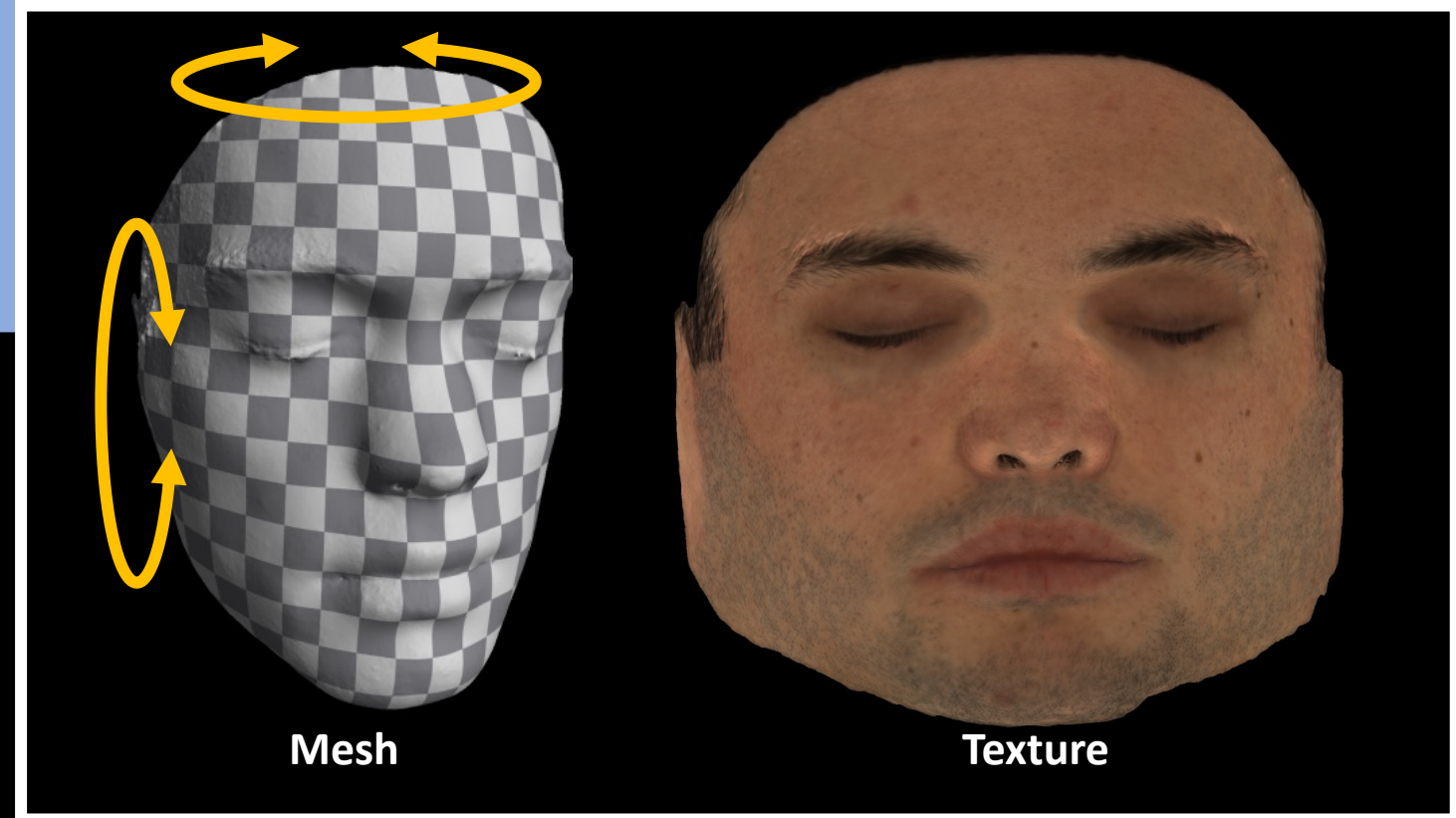


# Optimization Strategy



Static stage

Initial mesh and  
texture

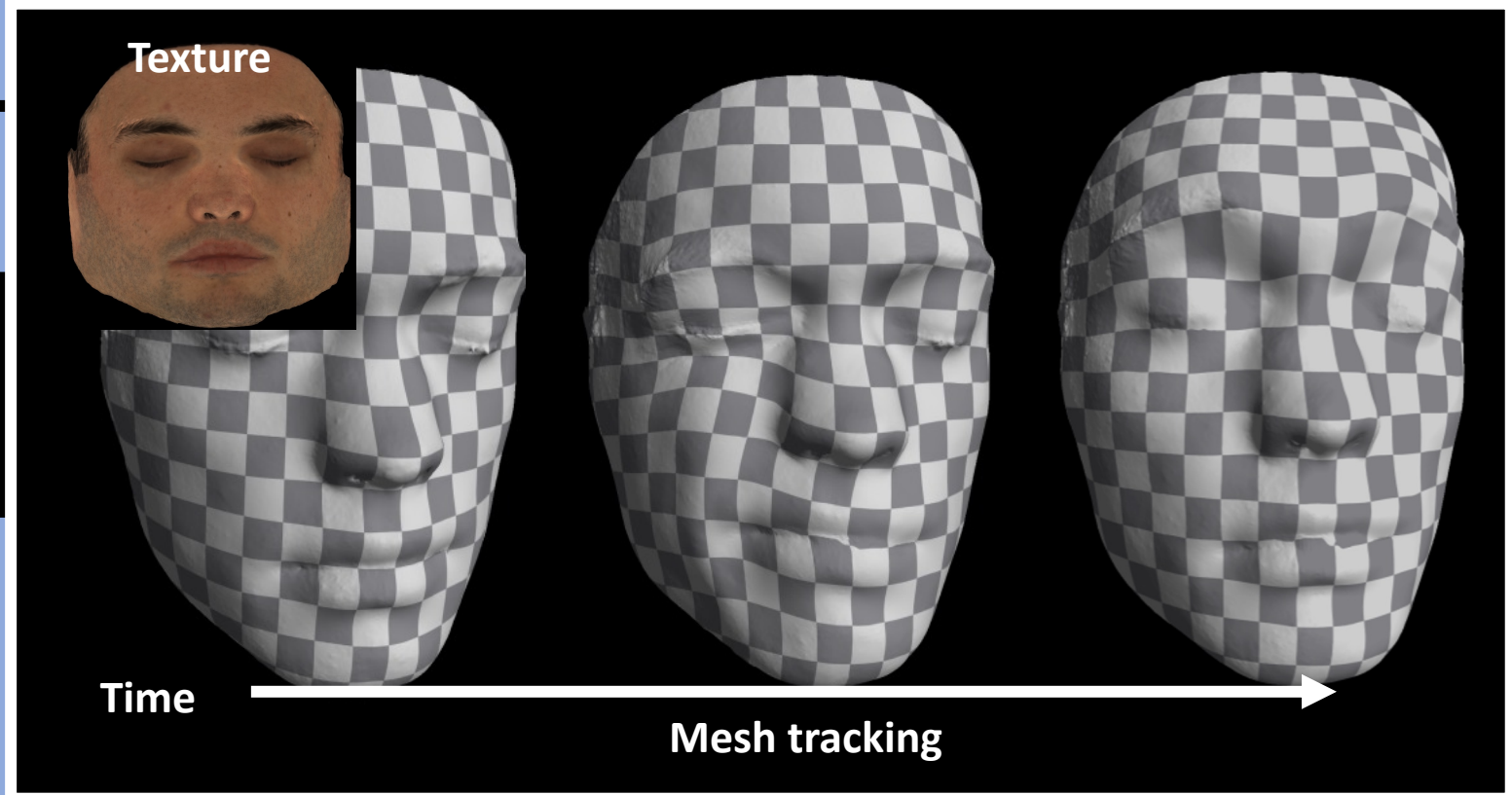


# Optimization Strategy



## Static stage

Initial mesh and texture



## Dynamic stage per frame

Per-frame tracked mesh and texture

# Optimization Strategy



## Static stage



Initial parameters

## Dynamic stage per frame



# Static Capture Stage



Hardware



Stereo camera module

Stereo camera module



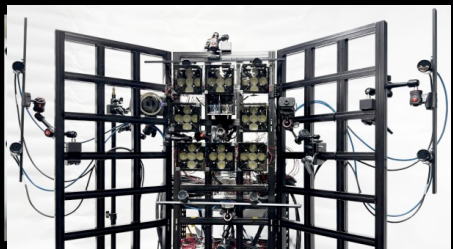
Dolby left polar. image

Dolby right polar. image



Stereo camera module

# Dynamic Capture Stage



Hardware



Stereo camera module

Stereo camera module



Dolby left polar. image



Dolby right polar. image

Stereo camera module



Stereo camera module

Stage: Dynamic capture

# Optimization of Polarimetric BSSRDF and Normal



$$\min_{\eta, \alpha_s, \alpha_{ss}, \rho_s, \rho_{ss}, \bar{\rho}_{sss}, H} \lambda_\psi \mathcal{L}_\psi + \lambda_{sss} \mathcal{L}_{sss} + \lambda_s \mathcal{L}_s + \lambda_\phi \mathcal{L}_\phi + \mathcal{L}_{\text{reg}}$$

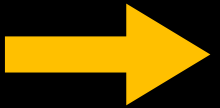
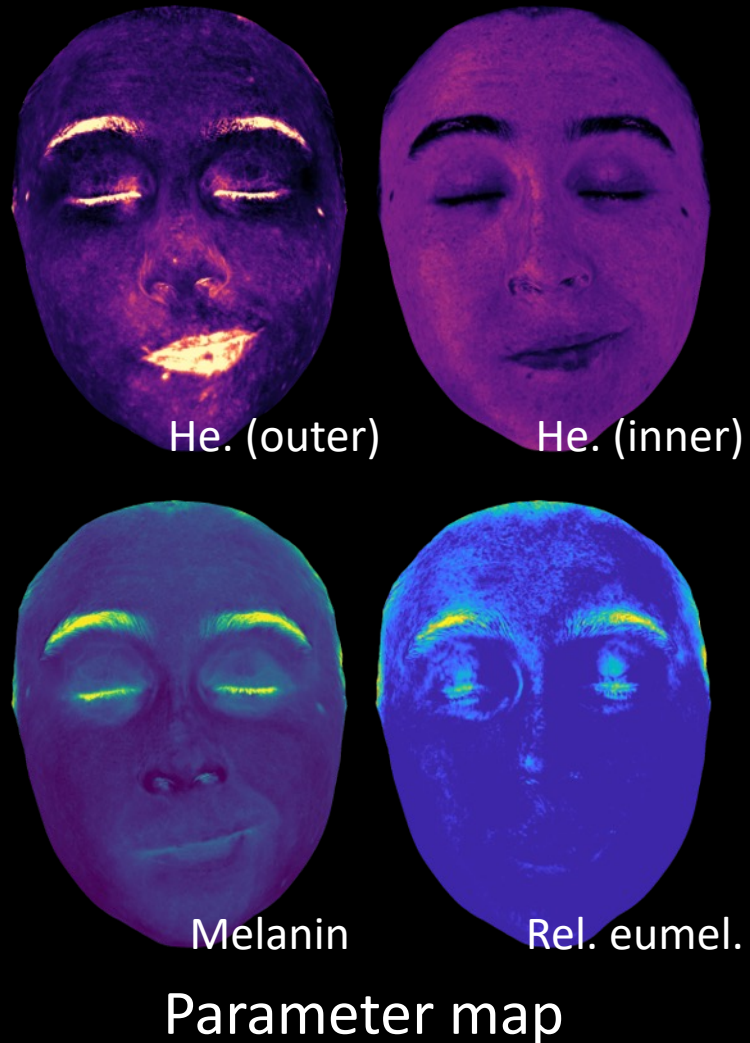
$\mathcal{L}_\psi$  : refractive index loss

$\mathcal{L}_{sss}$  : subsurface scattering loss

$\mathcal{L}_s$  : specular and single scattering loss

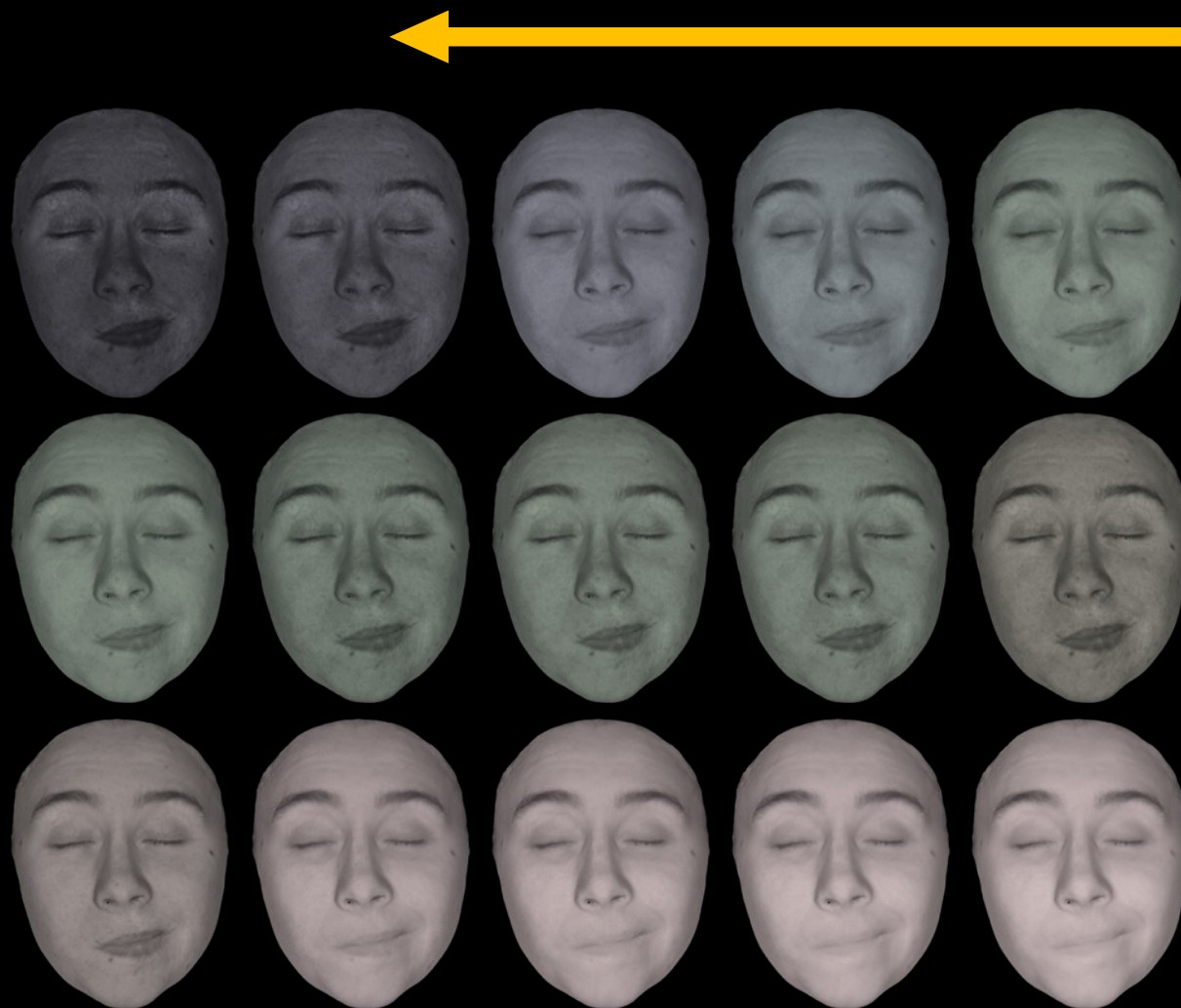
$\mathcal{L}_\phi$  : normal loss

# Optimization of Biophysical Parameters



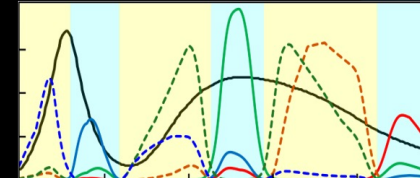


# Optimization of Biophysical Parameters



Gradient descent

Camera response



Dolby left

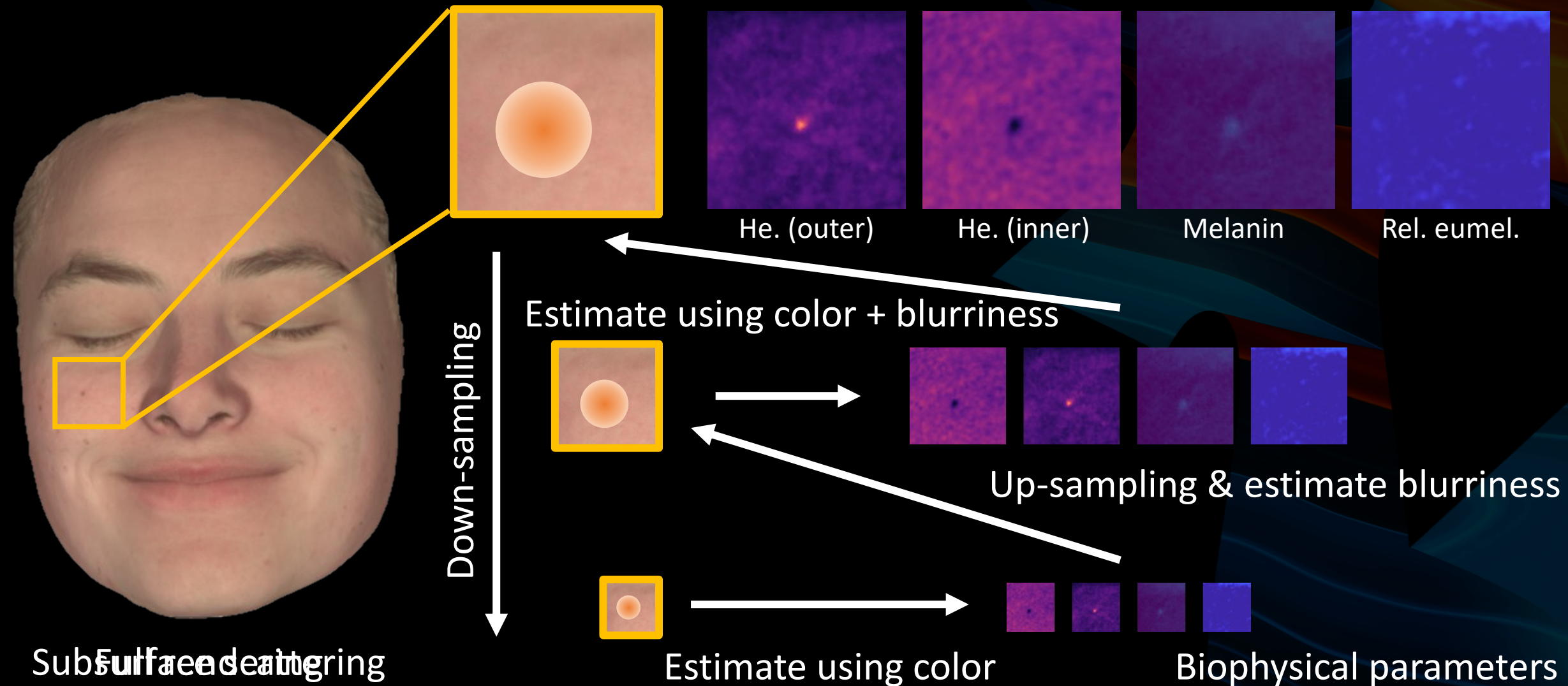


Dolby right

Target cameras

Rendering each wavelength (420nm ~ 670nm)

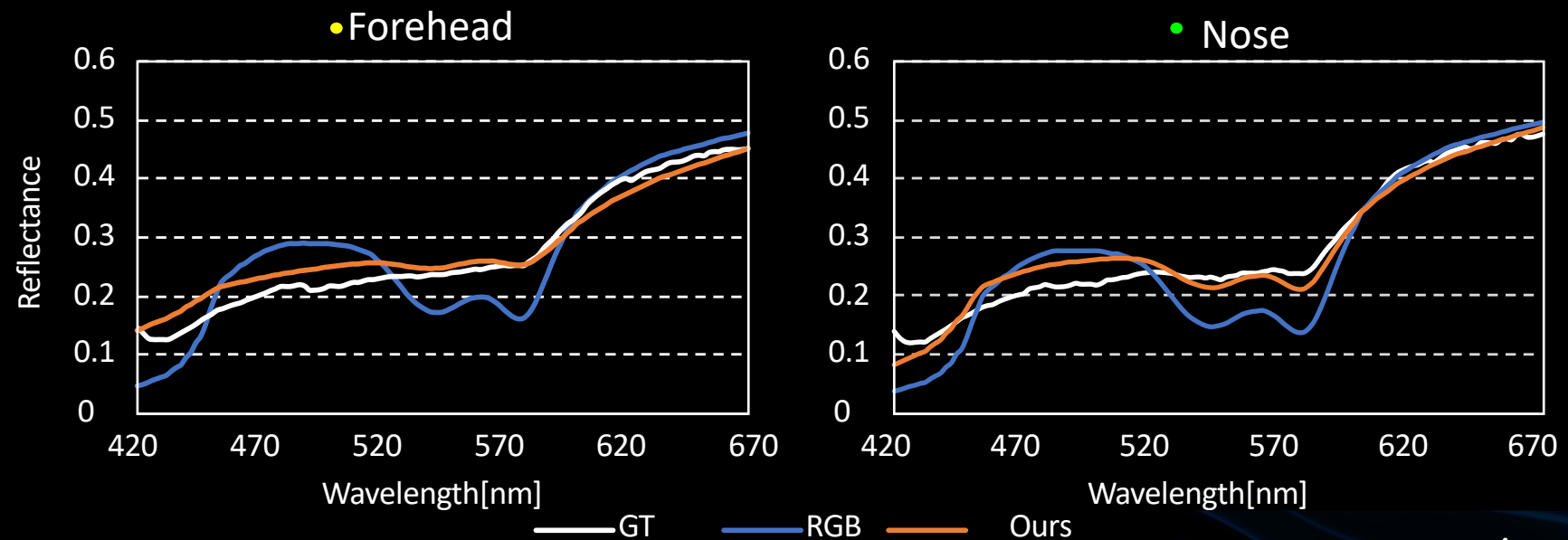
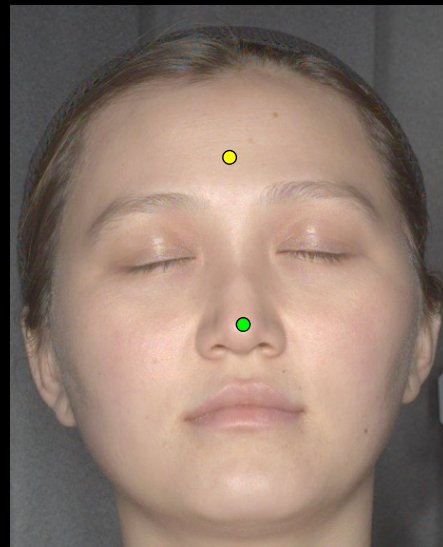
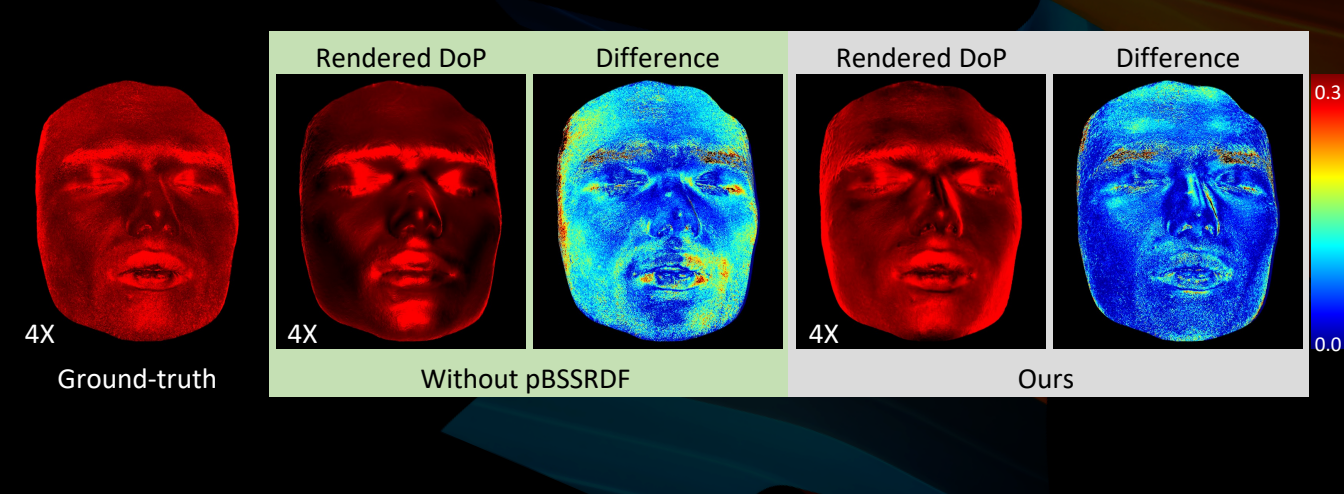
# Hierarchical Optimization of Biophysical Parameters



# Validation



Object	Material	$\eta_{gt}$	$\eta_{ours}$	Diff.
1	Red billiard	1.485	1.446	0.038
2	Green billiard	1.469	1.516	0.047
3	Blue billiard	1.504	1.503	0.001
4	White billiard	1.463	1.410	0.053
5	POM	1.462	1.447	0.015
6	Fake pearl	2.295	2.263	0.032
7	Yellow silicone	1.303	1.297	0.005
8	Pink silicone	1.177	1.211	0.034
9	White silicone	1.248	1.272	0.024
10	Light green silicone	1.343	1.311	0.032



↑↓  
Cam. Light



Rotating a linear polarization filter on the camera

↑↓ ←→  
Cam. Light

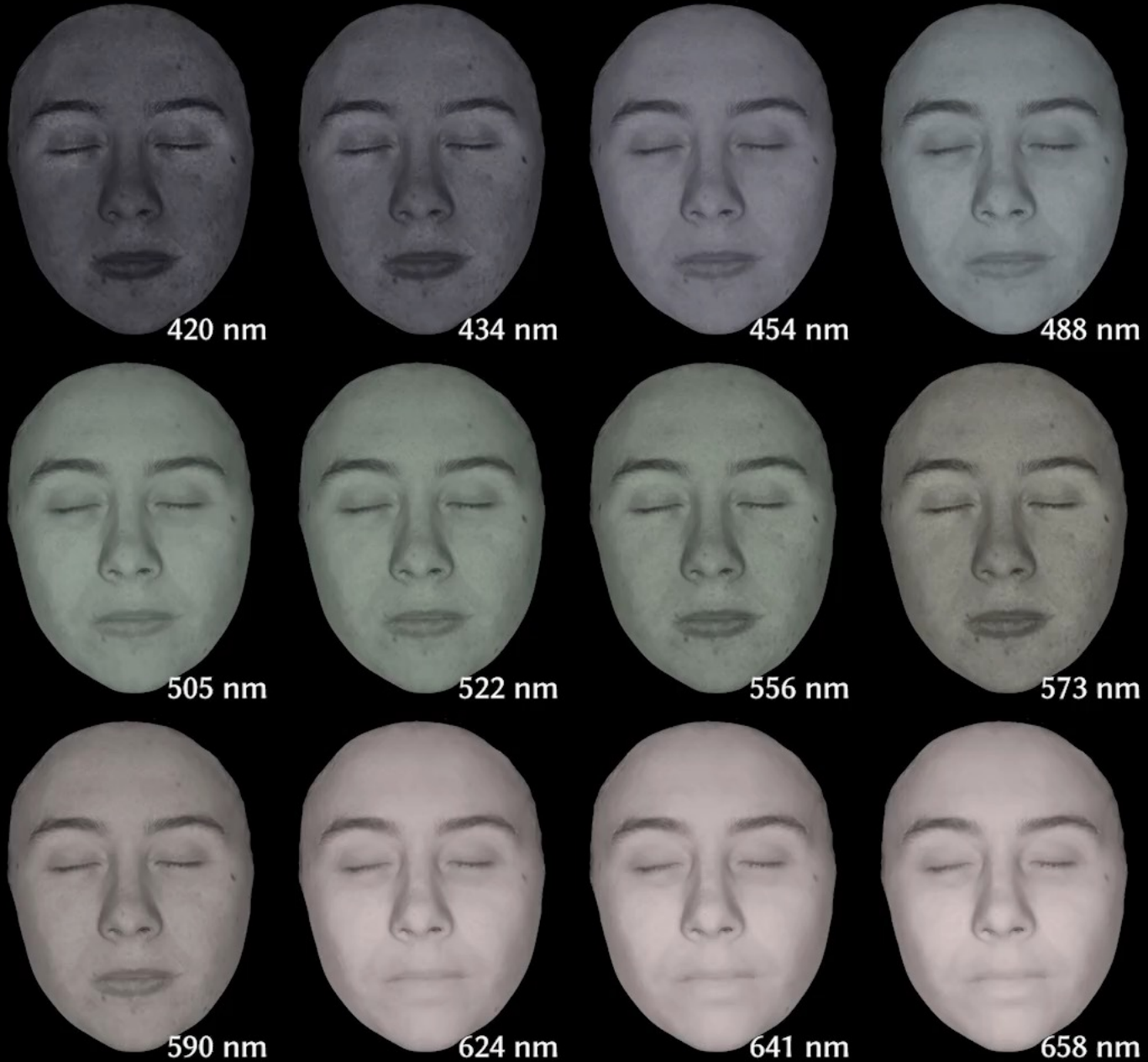


Rotating a linear polarization filter on the light

Polarization rendering



Full rendering



Multispectral two-layer subsurface scattering



Full rendering



Melanin



Hemoglobin (outer)

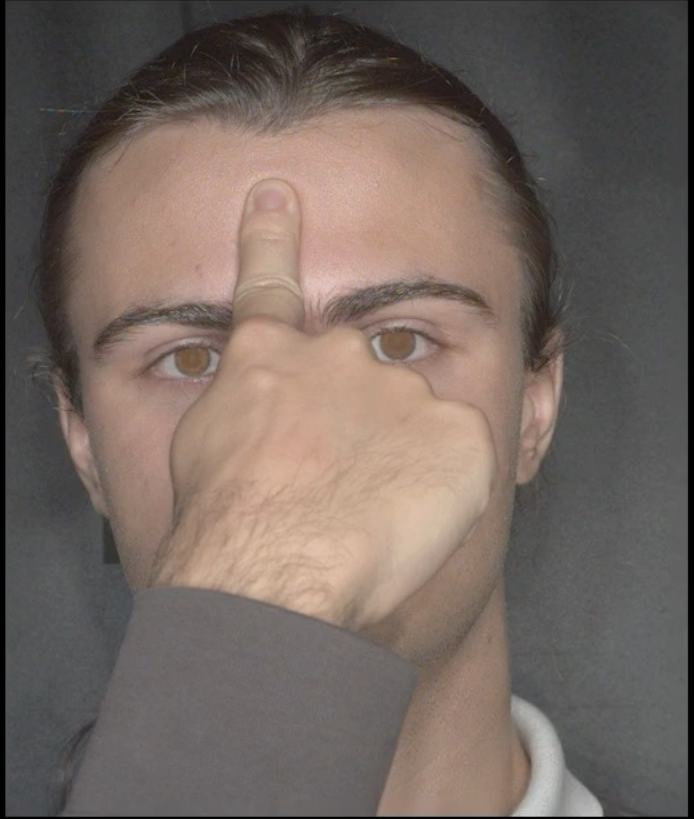


Relative eumelanin



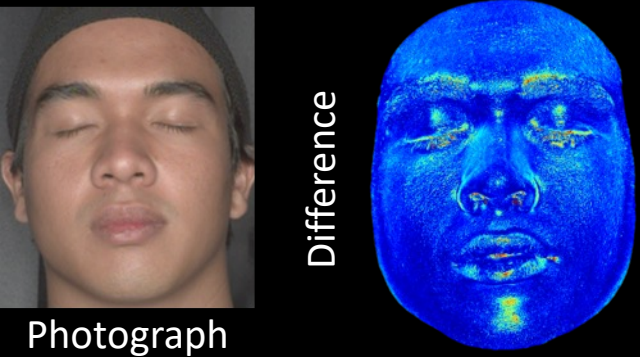
Hemoglobin (inner)



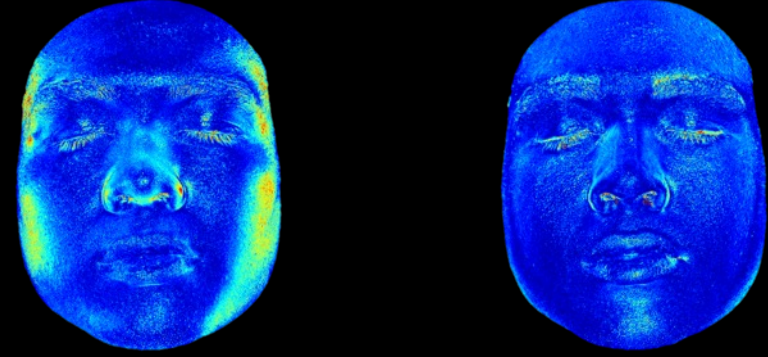


Pressing forehead

# Comparison



Photograph



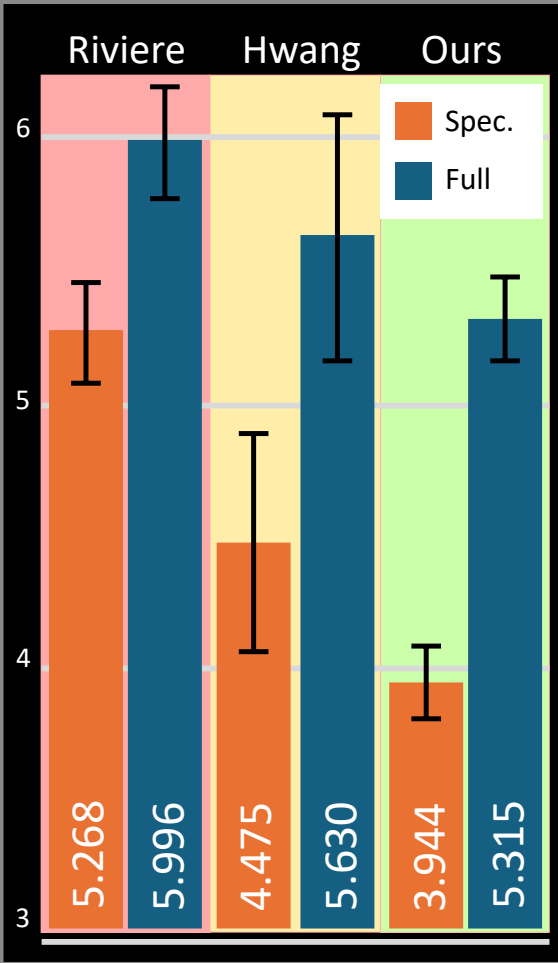
Full rendering (Riviere et al. [2020])



Full rendering (Hwang et al. [2022])



Full rendering (ours)



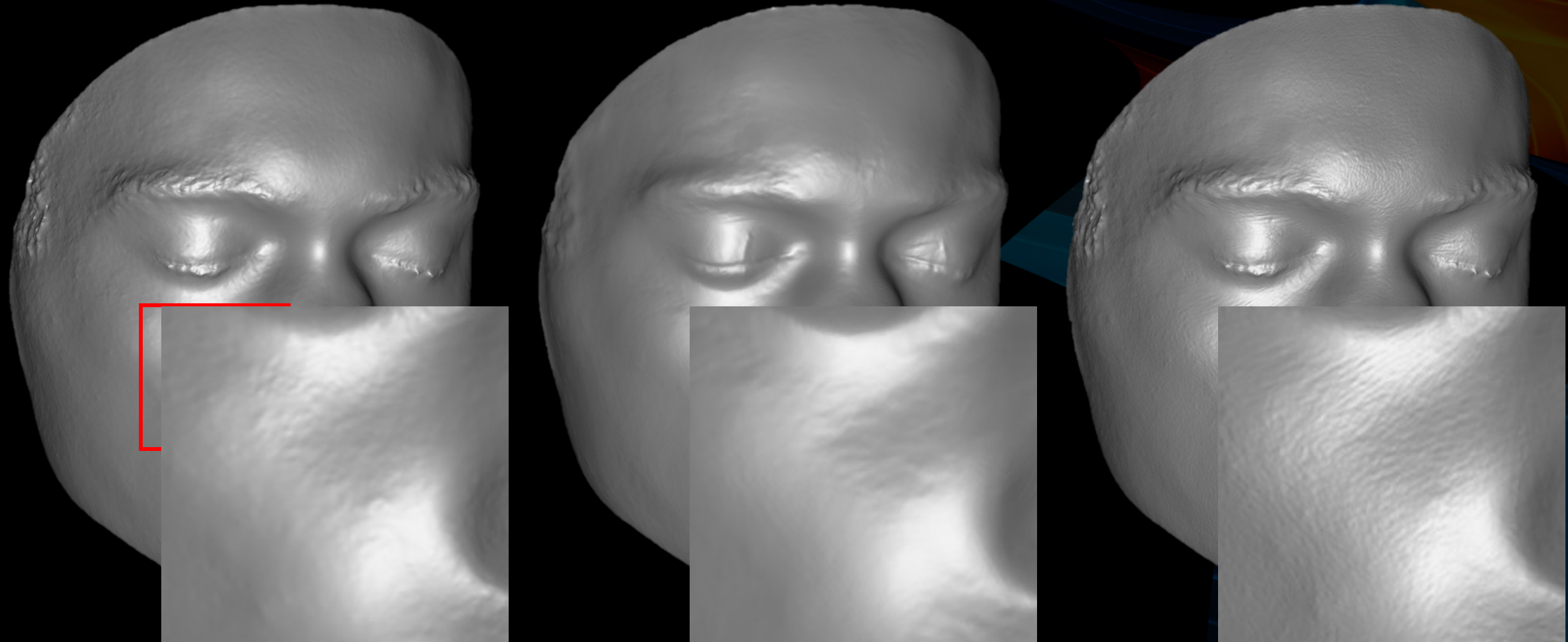
11 participants RMSE ( $\times 10^{-2}$ )



Organized by

koelnmesse

# Geometry Comparison

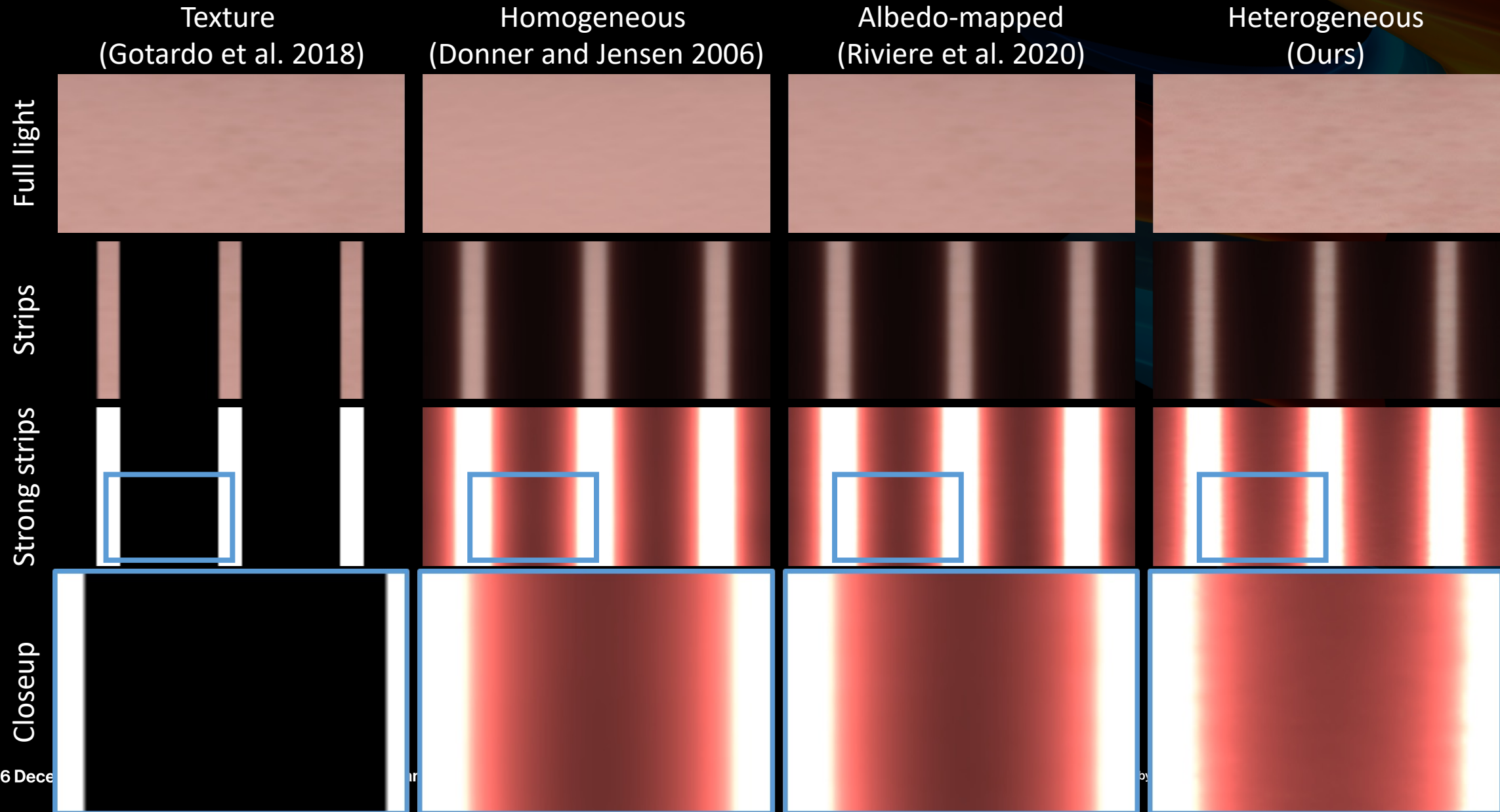


Stereo matching (Beeler et al. 2010)

Hwang et al. 2022

Ours

# Heterogeneous Multi-layered Translucent Materials



# Editing Face Parameters



Photograph



Rendering



Increase outer hemoglobin



Increase melanin



# Limitations and Future work



## Restrict by the two-layer skin model



Photo.



Render



He. (outer)



He. (inner)

- Future research could be on eyes and ears
- Darker skin cannot be estimated properly



## Quality restricted by hardware

- Low resolution and SNR compared to RGB
- Near-coaxial setup of camera and light



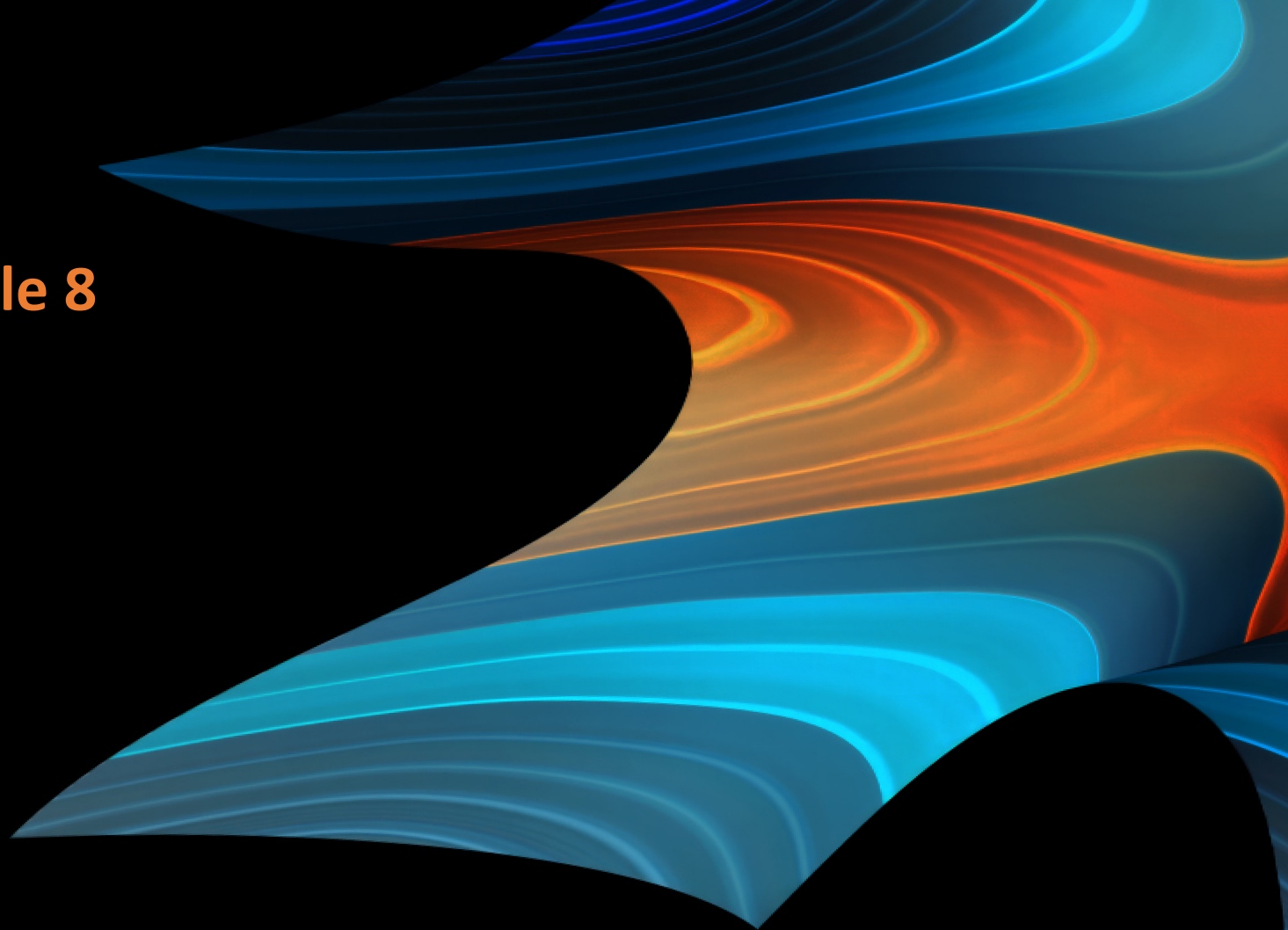
Interactive discussion at **Table 8**

Project Website



<https://vclab.kaist.ac.kr/siggraphasia2024>

**Thank you**



Sponsored by



Organized by

